

Cite this: *RSC Adv.*, 2015, 5, 42141

## Bioapplication of graphene oxide derivatives: drug/gene delivery, imaging, polymeric modification, toxicology, therapeutics and challenges

Md Nurunnabi,<sup>a</sup> Khaled Parvez,<sup>b</sup> Md Nafiujjaman,<sup>c</sup> Vishnu Revuri,<sup>c</sup> Haseeb A. Khan,<sup>d</sup> Xinliang Feng<sup>\*be</sup> and Yong-kyu Lee<sup>\*ac</sup>

Due to the wide range and various applications of graphene in multidisciplinary fields, such as electronics, solar cells, biomedicine, bioengineering, drug delivery, gene delivery and semiconductors, graphene and its derivatives have attracted most significant interest of diverse group of scientists in the last decades. Besides numerous applications in electrical and mechanical fields, their non-invasive biomedical imaging properties allow their wide-spread biological applications. Optical imaging probes play a pivotal role in early cancer detection, image based surgery, disease diagnosis and cellular imaging. Graphene has been widely studied in drug delivery systems due to its unique features and comparatively less/non-toxic properties in biological systems, thus promoting graphene quantum dots as potential organic optical imaging agents to substitute toxic cadmium or tellurium quantum dots. Many groups have also focused on different polymeric modification strategies to enhance the biocompatibility as well as the applications of graphene. In this review, we have summarized recent advances in graphene-based applications, and focused on the relation between chemical structure and polymeric modification with bio-safety issues. The lack of adequate biosafety studies and understanding of the interaction between graphene derivatives and biomolecules has hindered their progress in biomedical and biological applications. To proceed with biological applications of graphene derivatives, such as the development of graphene-based therapeutics and drug delivery systems, the research community must understand how graphene derivatives interact with cell lines and how they accumulate into cells. We also need to learn the fate of graphene derivatives *in vivo* once it invasively enters into a biological system.

Received 18th March 2015

Accepted 15th April 2015

DOI: 10.1039/c5ra04756k

[www.rsc.org/advances](http://www.rsc.org/advances)

<sup>a</sup>Department of Chemical and Biological Engineering, Korea National University of Transportation, Chungju 380-702, Republic of Korea. E-mail: leeyk@ut.ac.kr

<sup>b</sup>Max Plank Institute for Polymer Research, Ackermannweg 10, Mainz 55128, Germany

<sup>c</sup>Department of Green Bioengineering, Korea National University of Transportation, Chungju 380-702, Republic of Korea

<sup>d</sup>Analytical and Molecular Bioscience Research Group, Department of Biochemistry, College of Science, King Saud University, Riyadh 11451, Saudi Arabia

<sup>e</sup>Department of Chemistry and Food Chemistry, Technische Universität Dresden, 01062 Dresden, Germany. E-mail: feng@mpip-mainz.mpg.de



Md Nurunnabi is a postdoctoral fellow in Korea National University of Transportation (KNUT). He has received BS degree in Pharmacy at UODA (Bangladesh) in 2007, M. Eng in Chemical & Biological in 2010 and PhD in Polymer Science & Engineering in 2014 from KNUT. He has also served around 3 years in industries (2010–2012) as a research scientist and around 6 months (2013) at the University of Utah

as a visiting scholar. His research interests involve the development of a biocompatible and biosafe imaging agents for noninvasive diagnosis, polymeric drug delivery and oral gene delivery.



Khaled Parvez obtained his MSc in Polymer Science & Engineering from KNUT in 2010. He received his PhD degree in chemistry in October 2014 from the Max Planck Institute for Polymer Research (MPIP) under the supervision of Prof. Klaus Müllen. His current research interests revolve around the chemical synthesis of graphene and graphene based materials, especially for electronics and energy storage devices.

## 1. Introduction

Nowadays, carbon based materials, especially graphene and graphene derivatives such as graphene oxide (GO), reduced graphene oxide (rGO) and graphene quantum dots (GQDs), have attracted considerable interests for various interdisciplinary sciences that span a variety of disciplines including chemistry, physics, material sciences and nanotechnology.<sup>1</sup> Moreover, graphene and its derivatives are expected to revolutionize technological advances in electronics, ultrafast computing, and solar energy harvesting. Recently, graphene has also been proposed for biomedical applications such as drug delivery, biomedical imaging and anticancer therapy.<sup>2</sup> However, the actual application of any nanomaterial in biology and medicine is decided critically by its biocompatibility. Although, many graphene derivatives have been widely considered in various electronic devices, very few of them have been considered for biological applications. Though graphene-based derivatives have been considered for various biological applications such

as tissue engineering, bioengineering, drug delivery, gene delivery, optical imaging and therapeutics, to the best of our knowledge, none of the graphene derivatives have been considered for clinical trials yet.<sup>3</sup> Issues related to toxicity and bio-safety became pertinent as soon as graphene-based derivatives were used for biological applications.<sup>1</sup>

Graphene materials consisting of solely carbon are known to be non-toxic; however, it is a matter of serious concern to know how carbon derivatives like graphene decompose in a biological system and how long it takes to excrete them from the biological system.<sup>2</sup> However, during fabrication, graphene or sources of graphene usually undergo several chemical treatment processes for functionalization, including doping with metals, oxidation, introduction of functional groups and also reduction.<sup>4</sup> This indicates that some of the graphene derivatives considered for bio-applications contain metals and/or impurities other than carbon. For example, graphene quantum dots contain around 10% to 40% oxygen and 60% carbon. The presence of excess oxygen is one of the principle features that enhances the



*Md Nafiujjaman received his BS degree in Pharmacy from UODA in 2009 and M. Eng in Chemical & Biological Engineering from KNUT in 2013. Currently, he is pursuing doctoral degree in Green Bio engineering department at KNUT and expecting to receive graduation by 2016. His research interests focus on the fabrication of hybrid nanomaterials for therapy and diagnosis in Prof. Lee's lab.*



*Xinliang Feng joined the group of Prof. Klaus Müllen at the MPIP, where he obtained his PhD in 2008 and later on was appointed as a group leader. In 2011, he was appointed as a professor at Shanghai Jiao Tong University and as the director for the Institute of Advanced Organic Materials. He is also a full professor in Technical University of Dresden since 2014. His current scientific*

*interests include graphene, two-dimensional nanomaterials, organic conjugated materials and carbon-rich molecules and materials for electronic and energy related applications. He has published more than 210 peer-reviewed articles and has an h-index of 46.*



*Vishnu Revuri received his Masters in Medical Nanotechnology from SASTRA University, India in 2013. He later joined as a visiting researcher at the premier Biosensors and Bioelectronics Centre, Linköping University, Sweden. In 2014, he joined Prof. Yong-kyu Lee's lab at KNUT as a PhD student. His research is focused on designing novel mucoadhesive non-viral vectors for oral gene therapy.*



*Yong-kyu Lee is an associate professor of Chemical & Biological and Green Bioengineering Department at KNUT. He has received his MSc and PhD from GIST (Korea) in 1999 and 2003, respectively. He is the PI of Nano Biomedicine Laboratory at KNUT and founder of two start-ups, where he is leading various research projects on drug delivery, material chemistry, biomedical engineering,*

*tissue engineering, nanomedicine and coating technology. He has authored more than 60 high-impact-journal articles and has acquired 10 patents.*

solubility of graphene quantum dots and impart optical properties to them. Moreover, different graphene derivatives have different chemical properties with different functionalities and applications, thus they exert different toxicities.<sup>5</sup>

Though very limited studies have recently been conducted to discern the mechanisms of toxicology of graphene derivatives, especially of GO due to oxidative stress; no universal mechanism has been established yet.<sup>6,7</sup> In this review, we have summarized applications of graphene derivatives, polymeric modifications and toxicological investigations based on recent reports. We have also pointed out our perspective on the challenges of graphene derivatives for biological application and proposed ways to overcome these limitations (Fig. 1).

### 1.1. Graphene and graphene derivatives

Graphene consists of  $sp^2$  hybridized carbon atoms arranged in a honeycomb lattice and their electrons participate in aromatic conjugated domains. The remarkable physical, chemical and electronic properties of graphene and its derivatives has led to a wide range of applications such as in flexible displays,<sup>8</sup> light emitting diodes,<sup>9</sup> photodetectors,<sup>10</sup> batteries,<sup>11</sup> and supercapacitors.<sup>12,13</sup> In addition, graphene is considerably used for drug delivery, tissue engineering, stem cell research and biomedical imaging.<sup>1</sup> Several synthetic approaches, such as chemical vapor deposition (CVD),<sup>14</sup> micromechanical exfoliation,<sup>15</sup> liquid-phase exfoliation,<sup>16</sup> chemical<sup>17</sup> and electrochemical exfoliation,<sup>18,19</sup> have been applied in the preparation of graphene and its derivatives. The most notable of them is

GO–graphene sheets derived with oxygen-containing functional groups. GO is obtained by the widely used Hummers method, which uses potassium permanganate in concentrated sulfuric acid to oxidize graphite. Therefore, an individual GO sheet can be viewed as graphene decorated with oxygen functional groups on both sides of the plane and edges, where hydroxyl and epoxy groups decorate the basal plane, whereas carboxyls, carbonyls, lactones and quinones are located primarily at the edges. The oxygen containing functional groups in GO can also be removed by reducing agents such as hydrazine to produce rGO.<sup>20</sup>

In bioapplications, both oxidized (*i.e.* GO) and reduced (*i.e.* rGO) graphene are found to be feasible for drug delivery and therapeutic applications. The principle advantage of using GO over other carbon-based materials is its more reliable aqueous dispersibility and colloidal stability. The physicochemical characteristics of GO render it as a chemically versatile template with a high surface-to-volume ratio, which can be adjusted for facilitating a variety of biomedical applications such as imaging and cancer therapy. Apart from GO, graphene and reduced graphene oxide (rGO) have been found to be promising photosensitizing agents for photo-ablation because they generate heat upon irradiation.<sup>1,2</sup>

### 1.2. Graphene quantum dot

GQDs are a nano form of GO that have smaller size, zigzag shape and quantum confinement properties, and thus show band gap mediated and size tunable optical properties. The synthesis of GQDs has gained pre-eminence due to their strong quantum confinements, size dependent and edge sensitive photoluminescence properties. Different synthesis routes have been employed to tune their size and photoluminescence properties.<sup>21</sup> The synthesis methods of GQDs are broadly classified based on the approach used for tuning the size of GQDs to atomic precision as either (i) top-down approach or (ii) bottom-up approach.

The top-down approach is primarily based on defect arbitrated fragmentation, where different carbon precursors are exfoliated and decomposed under strenuous experimental conditions (such as concentrated acid treatment, strong oxidizing agents and elevated temperatures). However, these methods often suffer from defined control over the size and properties of the material.<sup>22</sup> On the other hand, the bottom-up approach exploits the use of polycyclic aromatic compounds to achieve an exquisite control over size and shape, and precisely regulate the physicochemical properties of the material. Bacon *et al.* briefly summarized different routes to synthesize GQDs.<sup>23</sup> Hydrothermal cutting is the simplest, most efficient and prevalent method used to synthesize GQDs and often employed in large scale batch production. Moreover, GQDs synthesized by this method have a plethora of oxygenated groups that assist in their aqueous dispersion and surface modifications. Pan *et al.* expounded the mechanism of GQDs synthesis from graphene sheets under hydrothermal treatment. They postulated that epoxy and carboxyl groups in the oxidized graphene sheets are labile and easily targeted under hydrothermal conditions for cutting. They also observed the



Fig. 1 The scheme represents the wide range bioapplications of graphene derivatives. Graphene, graphene oxide, reduced GO and graphene quantum dots can be fabricated from a carbon source and used in various bioapplications such as drug delivery, scaffolds in tissue engineering, optical imaging (*in vitro*, *in vivo*), therapy, biosensing and gene delivery.

pH-dependent photoluminescence properties of GQDs.<sup>24</sup> Luo *et al.* studied the effect of different oxidizing groups on the photoluminescence properties of GQDs. Their results showed a 2-fold increase in quantum yield compared to the precursors.<sup>25</sup> Feng *et al.* synthesized reduced graphene quantum dots (rGQDs) by a hydrazine reduced solvothermal method. They have shown that the reduction of GQDs prevented non radiative electron-hole recombination and the formation of pyrazole rings at the edges enriched their PL properties over pristine GQDs.<sup>26</sup> Zhang *et al.* used electrochemical exfoliation methods to synthesize GQDs for stem cell labelling. Production of O and OH radicals during anodic oxidation channeled the electrochemical trimming of carbon nanocrystals.<sup>27</sup> Ananthanarayanan *et al.* also used this method to synthesize GQDs for the detection of Fe<sup>3+</sup> ions.<sup>28</sup> Moreover, the magnetic properties of Fe<sup>3+</sup> ions resulted in the formation of GQD aggregates, which could be used as contrast agents for MRI. Luk *et al.* used the microwave-aided synthesis of PANI-GQDs for photonic devices. The functionalization of the GQD surface created emission traps and charge trapping sites at their surface states, which could enhance the electrical and optical properties of the films.<sup>29</sup> Other methods, such as nanolithography, ultrasonication and plasma assisted GQD synthesis, have also been used.<sup>30,31</sup>

Bottom-up fabrication strategies fostered the size controlled synthesis of GQDs with a molecular level precision with fine-tuned physicochemical properties. However, these methods are impeded due to their complex synthetic phases and small scale production. Yan *et al.* conducted a step-by-step organic synthesis of water soluble GQDs for solar cells using polyphenylene dendritic carbon precursors stabilized by 2',4',6'-tri-alkylphenyl groups.<sup>14</sup> Lu *et al.* synthesized ruthenium catalyzed GQDs from C60s. Ruthenium not only functioned as a catalyst but also acted as a template for the ring opened C60 clusters. Thermally activated diffusion led to the formation of GQDs from coalesced clusters on ruthenium with shear precision (Table1).<sup>32</sup>

## 2. Bioapplication of graphene derivatives

### 2.1. Current limitations in biomedical diagnosis and prospects of graphene derivatives

Early stage diagnosis techniques play a vital role for treating disease with minimal costs and improving treatment outcomes.<sup>1</sup> A feasible, cost effective and reliable early detection and diagnosis technology could enhance and extend the lifetime of patients.<sup>35</sup> However, existing *in vivo* diagnostic technologies, such as MRI and computed tomography (CT) scan, are expensive and inaccessible to the majority of patients. Moreover, existing *in vitro* diagnostic technologies such as biosensors are not yet ready to be used in the clinic. The development of cost effective and ideal contrast agents could overcome these barriers and accelerate the development of molecular imaging systems that can be used in biomedical diagnosis.<sup>36</sup>

Recent advances in nanomaterial based strategies for therapy and diagnosis have been very promising for the early

stage diagnosis and treatment of many diseases and infections.<sup>37</sup> Nanoparticle based therapies are able to overcome many of the existing barriers for cancer therapy because they enable the early detection and targeting of specific cells whilst minimising toxicity, and they are cost effective.<sup>38</sup> Many studies have revealed that early cancer detection either *in vitro* or *in vivo* could minimise treatment costs by 50% and the risk of death could be reduced by 60%.<sup>39</sup> *In vitro* analysis techniques are not yet an optimised or reliable way to detect biomarkers in the blood stream. Therefore, non-invasive imaging technologies, such as optical imaging, magnetic resonance imaging (MRI), positron emission tomography (PET) and X-ray computed tomography (CT scan) play vital roles in early stage diagnosis in deep tissue and organs.<sup>40</sup> However, the cost of current analytical tools is highly expensive due to the cost of contrast agents and imaging equipment. Previously, our group as well as other groups have reported that semiconductor QDs are more appropriate for optical imaging compared to organic dyes (such as rhodamine and cyanine) due to their unique properties (ultra nano-size, photo quenching stability, sharp emission and size variable excitation spectrum).<sup>41–43</sup> However, the toxicity of heavy metals, such as cadmium (Cd), tellurium (Te) and selenium (Se), is a major concern for their biological application. Due to serious toxicity, QDs have not been approved for clinical investigation, despite being studied for over a decade.<sup>44</sup> Recently, upconversion nanomaterials emerged as a new alternative to address the issues related with the impaired tissue penetration depths of light sources. Their unique property of emitting high energy photons upon low energy NIR excitations and easy surface modifications amplified their *in vivo/in vitro* imaging and PDT applications.<sup>45,46</sup> However, some studies report that they have low quantum yields and inaccurate surface modifications, which result in their uptake by the reticuloendothelial system and rapid clearance from the body. Moreover, biodistribution and toxicity evaluations are required to ensure their treatment in clinical applications.<sup>47</sup>

Current noninvasive imaging technology is an expensive way for detecting diseases due to the cost of contrast agents and imaging equipment, which limits its widespread application.<sup>48</sup> Because it is easy to fabricate the functional derivatives of graphene-based materials, they are known to be cost effective, nontoxic and stable imaging contrast agents used for *in vitro* and *in vivo* molecular imaging and biomedical diagnosis. The development of a cost effective, biocompatible, target specific, nontoxic and water dispersible graphene-based nanoparticles could solve many current problems in biomedical diagnosis and molecular imaging presented by toxic quantum dots and less stable organic dyes.<sup>49</sup> The newly developed multifunctional and biocompatible graphene nanoparticle can be widely used as optical imaging contrast agents as well as photo therapy for treating cancer. Photoluminescent GQDs can also be used to develop photoluminescence based biosensors for biomarker detection through surface plasmon resonance strategies.<sup>49</sup> Moreover, the fabrication of photo-tunable graphene nanoparticles with different colors from carbon fiber is comparatively easier. Some research groups have also focused on *in vitro* and *in vivo* imaging feasibilities of GQDs in different cell lines

Table 1 Reported synthesis process of graphene quantum dots

| Synthesis method                       | Carbon precursor                      | Parameters  | Physicochemical properties               | Applications   | Ref. |
|--|---------------------------------------|---|--|--|------|
| Hydrothermal cutting                   | Carbon fibers                         | Temp: 100 °C  | Em: 440 nm; size: 4.3 ± 0.9 nm           | Optoelectronics  | 25   |
|  | Graphene sheets (thermal deoxidation) | Teflon-lined autoclave: temp: 200 °C; reaction time: 10 h   | Em: 440 nm; size: 9.6 nm                 | Optoelectronics  | 24   |
|  | CX-72 carbon black                    | Reflux method: temp: 200 °C; reaction time: 24 h  | Size: 15–18 nm; Em: 520 nm to 590 nm     | Optoelectronics  | 33   |
| Solvothermal method                    | Graphite powder                       | Solvent: dimethylformamide (DMF); Teflon-lined autoclave: temp: 200 °C; reaction time: 8 h  | Size: 3.8 nm; Em: 440 nm                 |  | 26   |
| Microwave-assisted solvothermal method | GO (Hummers method)                   | Solvent: DMF; microwave irradiation: temp: 220 °C; reaction time: 12 h  | Size: 1.5–4.0 nm; Em: 425 nm             | Electrocatalyst for oxygen reduction                     | 34   |
| Electrochemical exfoliation method     | Graphite rods                         | Current intensity range: 80–200 mA cm <sup>-2</sup> ; reducing agent: hydrazine; reaction temperature: room temperature; reaction time: 8 h | Size: 5–10 nm; Em: 540 nm                | Stem cell labelling                                      | 27   |
|  | 3D graphene (CVD: ethanol precursor)  | Electrolyte: 1-butyl-3-methylimidazolium hexafluorophosphate; temp: room temperature  | Size: 3 nm; Em: 440 nm                   | Ferric ion detection; MRI                                | 29   |
| Nanolithography                        | Graphene crystals                     | Electron beam lithography; mask: polymethylmethacrylate   | Size: 10 nm;                             | Molecular-scale electronics; single-electron transistors | 30   |
| Microwave assisted hydrothermal method | Glucose                               | Microwave power: 300 W; reaction time: 5 min  | Size: 3.2–11.9 nm; Em: 440–520 nm        | Photonic devices   | 28   |
| Ultra-sonication                       | Graphene                              | Reaction time: 12 h; furnace (temp: 350 °C; time: 20 min)   | Size: 3–5 nm; Em: 407 nm                 | Bioscience and optoelectronics                           | 31   |
| Plasma assisted                        | Graphene (methane; CVD)               | Plasma: nitrogen; RF power: 10 W; pressure: 120 mTorr   | Size: 3–7 nm; Em: 360–420 nm             | Photoelectrochemical hydrogen evaluation                 | 21   |
| Fullerene cage opening                 | C60                                   | Catalyst and template: ruthenium; temperature: room temperature   | Size: 2.7 nm                             | Ultrafast high-density spintronic devices                | 33   |
| Oxidative condensation                 | Polyphenylene dendritic precursors    | Stabilizing agent: (2',4',6'-trialkylphenyl)phenylborate; reaction medium: argon  | Size 13.5 nm; absorbance maximum: 591 nm | Solar cell sensitizers                                   | 14   |

and small animals, respectively, as well as observed the primary toxicity behavior of GQDs.<sup>50,51</sup> Their observations showed that the uncoated cationic GQDs aggregated in aqueous medium, and thus showed significant toxicity *in vitro* and *in vivo*. Therefore, to prevent aggregation, coating and surface modification with polymers have been carried out. Coating of GQDs with polydopamine greatly prevents aggregation, and the coated GQDs can be used for the delivery of drugs and genes through catechol medicated linkages.<sup>52</sup> Photosensitivity is another mentionable limitation of GQDs because they generate single oxygen upon irradiation with visible or UV light, thus cells and tissues surrounding the GQDs become affected by toxic singlet oxygen. However, this photosensitivity and the photodynamic properties of GQDs are turned toward positive approaches as therapeutics for treating diseases and wounds.

The chemical modifications of GQDs with biocompatible polymers enhanced the solubility of GQDs and made them feasible for both photo-cancer therapy and real time imaging for detecting the cancer cells/tumor. We modified the surface of

GQDs with polydopamine and hyaluronic acid to impart hydrophilicity and explore the feasibility of GQDs as multi-functional nanomaterials for cancer therapy and gene therapy.<sup>52</sup>

## 2.2. Graphene for drug delivery

Since their discovery as a bio-safe material, graphene has been explored as a carrier molecule in drug delivery research.<sup>1,2</sup> The large specific surface area of graphene enhances opportunities for multi drug delivery to the target site from the site of administration. Polymeric modification and conjugation strategies also enhance biocompatibility and circulation times *in vivo*.<sup>53</sup> Several studies have been conducted on the delivery of anticancer drugs, genes and peptides through graphene derivatives in the last couple of years.<sup>54–60</sup> Simple physisorption *via*  $\pi$ - $\pi$  stacking can be used for loading many hydrophobic drugs, such as doxorubicin and docetaxel, with antibodies for the selective killing of cancer cells. Owing to its small size, intrinsic optical properties, large specific surface area, low cost and useful non-covalent interactions with aromatic drug molecules,

graphene is a promising new material for drug delivery through the nano-carrier approach. The large specific surface area,  $\pi$ - $\pi$  stacking and electrostatic or hydrophobic interactions of graphene can assist in high drug loading of poorly soluble drugs without compromising potency or efficiency.

Joo and his group reported that PEGylated GO loaded doxorubicin *via*  $\pi$ - $\pi$  interactions shows promising real-time release of DOX from PEGylated GO at a specific loci after an external triggering by GSH.<sup>55</sup> Another research group reported that GO loaded with doxorubicin exhibits higher drug release at pH 5.3 due to the reduced interaction between DOX and the drug carrier.<sup>56</sup> GO loaded with DOX shows enhanced cellular toxicity and promising tumor growth inhibition, with almost 66% to 91% cell death.<sup>57-59</sup> Other chemotherapy drugs, such as

paclitaxel and methotrexate loaded on GO *via*  $\pi$ - $\pi$  stacking and amide bonds, exhibited amazing cancerous effect on lung cancer and breast cancer, which was resulted inhibition of about 66% to 90% tumour growth.<sup>60,61</sup> When ibuprofen, which is used as an NSAID, was conjugated with chitosan functionalized GO *via* amide linkages, the functionalized GO exhibited higher (20%) biocompatibility than GO sheets for CEM & MCF-7 cell lines.<sup>62</sup> GO loaded with a second generation photosensitizer chlorin e6 (Ce6) resulted in its higher accumulation in tumor cells, leading to a higher photodynamic efficacy upon irradiation.<sup>63,64</sup> Nano GO is another important material for the drug delivery research area. Nanographene oxide (NGO) is used as a novel and efficient nanocarrier for the delivery of water insoluble aromatic anticancer drugs into cells. The approach was,

Table 2 The application of different graphene derivatives for drug delivery

| Graphene derivatives | Drug         | Application  | Ref. |
|----------------------|--------------|--|------|
| GO                   | DOX          | <i>In vitro</i> : A549 cells<br><i>In vivo</i> : Cg-Foxn1nu/CrljOri nude mice<br>Results: released 15% to 20% increase                 | 55   |
| GO                   | DOX          | <i>In vitro</i> : drug release<br>Results: higher drug release at pH 5.3   | 56   |
| GO                   | DOX          | <i>In vitro</i> : HeLa cells and OCT-1 mouse osteoblasts<br><i>In vivo</i> : BALB/c nude mice<br>Results: 71% tumour growth inhibition | 57   |
| GO                   | DOX          | Results: pH-triggered controlled magnetic behaviour  | 58   |
| GO                   | DOX          | <i>In vitro</i> : SK3 cells<br>Results: enhanced cellular toxicity   | 59   |
| GO                   | Paclitaxel   | <i>In vitro</i> : A549 and MCF-7 cells<br>Results: 90%   | 60   |
| GO                   | Methotrexate | <i>In vitro</i> : MCF7 cells<br>Results: 66.1%   | 61   |
| GO                   | Ibuprofen    | <i>In vitro</i> : CEM and MCF7 cells<br>Results: about 95%   | 62   |
| GO                   | Ce6          | <i>In vitro</i> : KB cells<br>Results: 98%   | 63   |
| GO                   | Ce6          | <i>In vitro</i> : MGC803 cells<br>Results: 90%   | 64   |
| Nano-GO              | DOX          | <i>In vitro</i> : CEM.NK T-cells and Raji B-cells<br>Results: 80% cell growth inhibition   | 65   |
| Nano-GO              | SN38         | <i>In vitro</i> : HCT-116 cells<br>Results: 80% cell growth inhibition   | 66   |
| Reduced GO           | DOX          | <i>In vitro</i> : PC-3 and HeLa cells<br>Results: 80% cell growth inhibition   | 67   |
| Graphene nanosheet   | DOX          | <i>In vitro</i> : MCF-7cells<br>Results: the cytotoxicity enhanced gradually   | 68   |
| Graphene nanosheet   | DOX          | <i>In vitro</i> : U251 and 1800 cells<br>Results: 55%  | 69   |
| Graphene nanosheet   | DOX          | <i>In vitro</i> : A-5RT3 cells<br>Results: 90%   | 70   |
| Graphene nanosheet   | Methotrexate | <i>In vitro</i> : A549 cells<br>Results: 70.2%   | 71   |
| Graphene nanosheet   | 5FU          | <i>In vitro</i> : HepG2 cells<br>Results: 72% growth inhibition  | 72   |
| Graphene quantum dot | DOX          | <i>In vitro</i> : A549 cells<br>Results: 95%   | 73   |
| Graphene quantum dot | DOX          | <i>In vitro</i> : A549 cells<br><i>In vivo</i> : BALB/c mice<br>Results: 60%   | 74   |
| Graphene quantum dot | DOX          | <i>In vitro</i> : HeLa, A549, and HEK293A cells<br>Results: 60%  | 75   |

nano GO was first conjugated with PEG to obtain PEG-NGO. Further, doxorubicin (DOX) and camptothecin (CPT) analog, SN38 were conjugated by non-covalent  $\pi$ - $\pi$  interactions. These complex showed pH dependent drug release and prominent cytotoxicity levels in HCT-116 cell lines which was 1000 fold potential than CPT.<sup>65,66</sup> Kim *et al.* reported that near infrared (NIR) radiation, acidic pH and high intracellular concentrations of GSH favored intracellular cytosolic delivery of DOX. Cells treated with PEG and branched polyethylenimine (BPEI)-functionalized rGO (PEG-BPEI-rGO) nano-carriers exposed to near-IR irradiation encouraged endosomal disruption and consequent DOX release, which triggered cellular toxicity.<sup>67</sup> Graphene derivatives have been conjugated with biopolymers, such as gelatin and polyethylene glycol, as functionalizing agents for drug delivery applications. Gelatin and polyethylene glycol not only favoured the reduction of

graphene but also functionalized GNS, facilitating the loading of DOX onto GNS. The GNS-DOX complex also exhibited high toxicity towards U251, 1800 and A-5RT3 cells through endocytosis.<sup>68,69</sup> Poly NIPAM and other polymers have been used with graphene for loading various drugs such as camptothecin,<sup>70</sup> methotexate,<sup>71</sup> and 5-fluorouracil.<sup>72</sup> In the recent past, researchers have begun to synthesize smaller graphene derivatives, often referred as graphene quantum dots (GQDs). These GQDs exhibit intrinsic fluorescence, and are also used for theranostic purposes. Synthesized GQDs with different color emissions and loaded with anticancer drugs such as



Fig. 2 (A) Schematic illustration of  $^1\text{O}_2$  generation mechanisms by conventional PDT agents (left) and GQDs (right). (B) Fluorescence intensity of GQDs at 680 nm versus the  $\text{O}_2$  concentration in solution. (C) The dependence of the  $^1\text{O}_2$  quantum yield ( $Q_\Delta$ ) on the fluorescence intensity ratio at 680 nm ( $F/F^0$ ). Adapted with permission from ref. 80. Copyright © 2013 Nature publishing group. Simultaneous photothermal, photodynamic and optical imaging properties of GQDs (D), adapted with permission from ref. 35. Copyright © 2014 American Chemical Society.

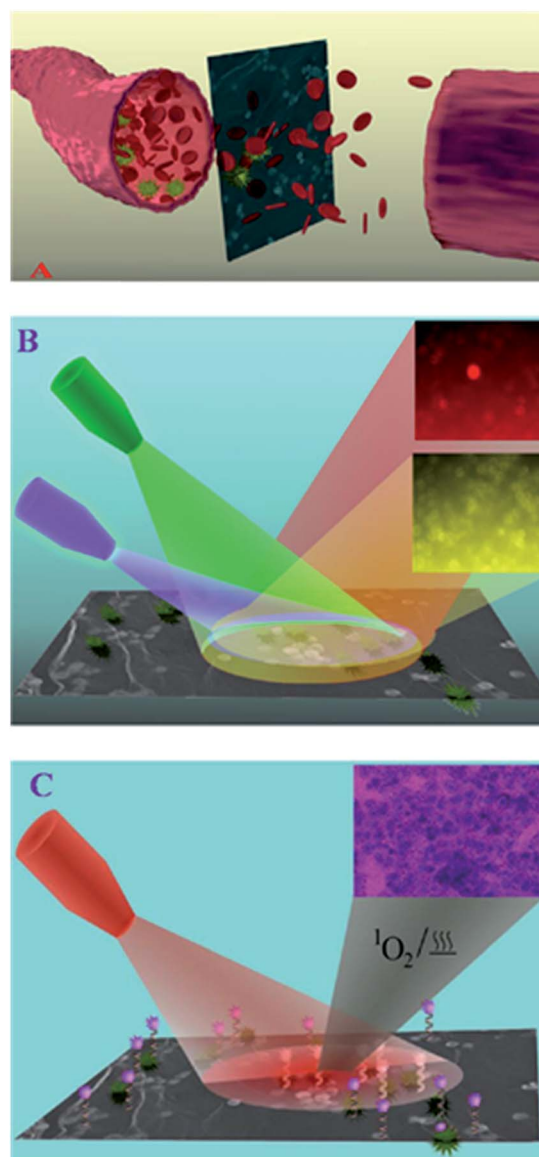


Fig. 3 (A) Schematic representation showing EpCAM antibody and A9-aptamer-attached theranostic GO for the separation and capturing of CTC from infected blood. (B) Schematic showing the label-free multicolor luminescence imaging of CTC using EpCAM antibody and A9-aptamer-attached theranostic GO. (C) Schematic showing that the theranostic GO can be used for combined synergistic treatment. Adapted with permission from ref. 83. Copyright © 2014 WILEY-VCH Verlag GmbH & Co. KGaA, Weinheim.

doxorubicin were reported to have an image-guided higher therapeutic efficacy of about 55% to 90% cell growth inhibition (Table 2).<sup>73–75</sup>

### 2.3. Graphene for tissue engineering

Functional carbon-based nanomaterials have become important due to their unique combination of chemical and physical properties. In tissue engineering research, the selection of a scaffold plays a vital role in the design and development of a hydrogel with optimized properties such as conductivity, mechanical properties and elasticity. The selection of biocompatible and biomimetic scaffolds also plays a vital role in minimizing toxicity, which happens through the auto-immune system. Zhang *et al.* incorporated GO into poly(vinyl alcohol) hydrogels to improve the mechanical strength of the hydrogel.<sup>76</sup> More recently, researchers have turned their attention toward utilizing the multifunctional nature of carbon derivatives in engineering tissue scaffolds. Most notably, carbon materials have been employed in the fabrication of electrically conductive scaffolds. Most of the biomaterials used for tissue engineering applications are electrically insulating because they are made from nonconductive polymers.<sup>77</sup> Another study demonstrated a synthesis of self-assembled graphene hydrogel *via* a convenient one-step hydrothermal method. The inherent biocompatibility of the carbon materials in the self-assembled graphene hydrogel is attractive in the fields of biotechnology and electrochemistry for applications such as tissue scaffolds and bionic nanocomposites.<sup>78</sup> Graphene derivatives are found to be a promising composite material in tissue engineering due to their non-significant toxicity, natural source, and excellent thermal and electrical conductivity.

### 2.4. Graphene as a photomedicine

Non-uniform coverage of oxygen functional groups in GO sheets results in ordered small  $sp^2$  clusters, which are isolated within  $sp^3$  C–O matrix. The presence of finite molecular  $sp^2$  clusters within a  $sp^3$  matrix can lead to the confinement of  $\pi$ -electrons in GO. The radiative recombination of electron–hole pairs in such  $sp^2$  clusters can give rise to fluorescence.<sup>79,80</sup> The size of the local  $sp^2$  cluster determines the local energy gap, and therefore the wavelength of the emitted fluorescence. An emission in the UV-visible region can occur from  $sp^2$  clusters with sizes of less than 1 nm. On the other hand,  $sp^2$  domains that are larger than 2 nm possess smaller gaps and may account for red to near-IR emission. The strong optical absorbance of GO in the near-IR region has been applied for *in vivo* photothermal therapy.<sup>35</sup> Many research groups have reported on the application of graphene and its derivatives for cancer therapy. For example, polyethylene glycol functionalized GO enhanced therapeutic efficacy and showed a high cellular uptake.<sup>81</sup> Promising therapeutic outcomes were observed from PEG–GO conjugates through many studies, which are attributed to the fact that the reduced GO has better photoablation properties over the non-reduce graphene derivatives.<sup>81</sup> To obtain a synergistic and enhanced therapeutic efficacy for cancer treatment, a combination of therapeutic multifunctional nanoparticle was

designed. The PEG–GO nanoparticle conjugated with doxorubicin enables a combination of photothermal and chemical therapy for cancer treatment. Recent results show that GQDs have the highest singlet oxygen generation capacity over conventional photosensitizers (PSs) due to their multistate sensitization. In comparison to a conventional PS, GQDs exhibited enhanced  $^1O_2$  quantum yields. This enhancement was envisaged to be based on the generation of singlet oxygen species during their transition from an excited state to the triplet state in the visible region (below 636 nm), which is not seen in conventional PS (Fig. 2).<sup>80</sup>

### 2.5. Theranostics: a combination of diagnostics and therapy

Because graphene and GO, especially graphene quantum dots, have a wide range of excitation and emission properties, as investigated previously, many research groups have mainly aimed to introduce a novel and new graphene-based optical imaging agent that can be considered as a unique contrast agent for deep tissue and cell imaging, and cancer therapy as well. Previous studies on photoluminescent graphene demonstrated several methods for producing different tunable colors from NGO.<sup>37</sup> Acid exfoliation, tunable laser irradiation, electronic beam irradiation, autoclaving and many other methods have been reported for the fabrication of photoluminescent graphene in the last couple of years. However, the combined application of graphene for therapeutic and imaging has yet to be reported.<sup>40</sup> To acquire an efficient theranostic effect, the material should facilitate multimodal imaging with suitable surface areas that enable them as a surface to adsorb the drugs and afford sufficient surface modifications to assist in site specific targeting. Though different theranostic systems have been designed, they often lack some of the abovementioned qualities. Because cancer cells have a tendency to develop an intrinsic multiple drug resistance (MDR) profile, there is a need to design multimodal therapeutic systems with effective targeting. To overcome these impairments, scientists came up with the concept of synthesizing composite systems that satisfy all the above mentioned complications. Because GO has unique properties and is easy for functionalization, these materials were chosen as an optimal material to design theranostic nanocomposites. Several graphene-based nanocomposite formulations have been synthesized and envisaged as ideal theranostic and multifunctional nanomedicines. Recently, peptide and magnetic GO functionalized mesoporous silica nanomaterials have been synthesized to selectively target glioma cells. GO enhanced the drug loading capacities of the system and featured a pH responsive drug release assisted photothermal treatment. Moreover, these materials gained dual receptor mediated and magnetic guided drug transport with MRI.<sup>82</sup> Another interesting property of GO nanosheet-based theranostic materials is their wavelength dependent photoluminescence. This exhilarating feature could be either due to the wavelength dependent fluorescence from OH groups in GO or solvent relaxation times due to the excited GO, which could be compared to the fluorescent times.<sup>83,84</sup> Tagging a photosensitizer with an aptamer to the magnetic GO nanosheets enables



multi-luminescent label free cell imaging with photothermal and photodynamic MRI guided therapy.<sup>85</sup> Graphene-based nanomaterials have also been used as a surface enhanced Raman scattering (SERS) material to selectively deliver and monitor drug release from the carrier system. Because piperazine ring has a stronger affinity for the {100} planes of gold, graphene can be preferred as an optimal material to seed and grow noble metals on their surface, thus creating an interface with non-thiolated molecules and generate adequate SERS signals. Because drug affinity to the GO can be reduced in acidic pH, these SERS signals can easily assist in monitoring drug release from the carrier.<sup>86,87</sup> Moreover, the presence of GO can assist in photothermal therapies to treat skin cancer (Fig. 3).<sup>88</sup>

## 2.6. Graphene for gene delivery

Graphene-mediated gene delivery is another emerging area of research that has been considered by research groups who are focusing on non-viral gene delivery. The majority of the scientific studies in this area have reported that graphene derivatives could be used as a promising carrier with high gene packing densities due to their large surface areas. Some reports also demonstrated that the graphene derivatives could overcome many barriers and increase gene accumulation through the targeting of specific cells, resulting in increased gene transfection. However, modifications of graphene derivatives with polymers are required to render cationic surface properties and facilitate electrostatic interactions with anionic oligonucleotides. Mostly polyethyleneimine (PEI), PEG and poly(sodium 4-styrenesulfonates) (PSS) have been considered for gene delivery through graphene derivatives.<sup>81,89,90</sup> Zhi *et al.* reported that layer-by-layer assembled GO carrying miR-21 simultaneously targeted siRNA and adriamycin and was able to overcome multidrug resistance.<sup>91</sup> The polymer associated with GO significantly enhanced cellular uptake in MCF-7 cells. Another study by Khademhosseini's group applied GO-based injectable hydrogels to host angiogenic genes and demonstrated the hydrogels to be a potential cardiac implant for vasculogenesis.<sup>92</sup> This invention can be widely used in tissue engineering research for generating blood vessels to circulate blood and nutrients for the cells located inside the hydrogel. The thermogenesis properties of rGO have been properly implicated by Kim *et al.*, where they showed that light sensitive rGO can be used to escape or overcome the barriers of current gene therapeutic strategies.<sup>93</sup> The translocation of a gene from cellular membrane to the nucleus is a hurdle due to the endosomal barrier between the routes. Though many strategies have been taken into consideration to overcome this barrier, progress is far away from expectations. This report has suggested that the heat generated through the irradiation of rGO helps to overcome endosomal escape, thus enhancing gene expression (Fig. 4).

## 3. Polymeric modification of graphene derivatives

Polymer nanocomposites based on graphene and graphene derivatives have found eminence in various biomedical

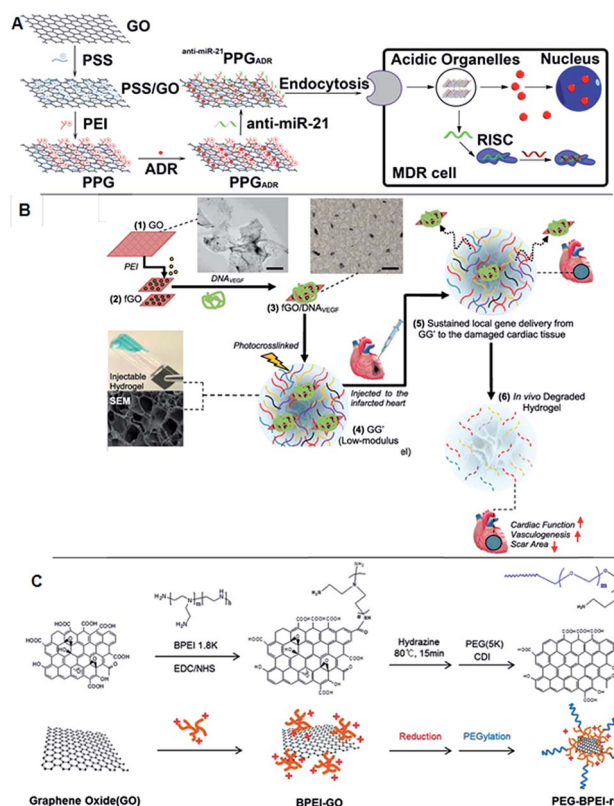


Fig. 4 Schematic of the fabrication of polyethyleneimine (PEI)/poly(sodium 4-styrenesulfonates) (PSS)/graphene oxide and multidrug resistance reversion (A) adopted with permission from ref. 91. The scheme represents the preparation of injectable hydrogel incorporating with PDNA and GO for acute myocardial infarction therapy (B). Adapted with permission from ref. 92, Copyright © 2013 American Chemical Society. Synthesis scheme of PEG-BPEI-rGO nanocomposite. BPEI-rGO was synthesized from BPEI-GO. To enhance the colloidal stability of BPEI-GO and BPEI-rGO, polyethylene glycol monomethyl ether (mPEG) was conjugated with 1,1'-carbonyldiimidazole coupling (C). Adapted with permission from ref. 93, Copyright © 2014 WILEY-VCH Verlag GmbH & Co. KGaA, Weinheim.

applications, *viz.*, tissue engineering, drug delivery and biosensors. GO-based nanomaterials have recently attracted considerable attention in the 2D carbon family for multifarious applications. The surface and the edges of GO possess hydroxyl and carboxyl groups that expedite easy functionalization and impart a dynamic change in the physicochemical properties of the composite materials. Moreover, higher surface areas and structural defects can foster interactions with the polymeric materials. Recent studies show that 2D graphene-based carbon nanomaterial reinforced polymer composites displayed enhanced mechanical properties over 1D carbon nanomaterials. Having a higher surface area with low aspect ratios and higher crosslinking densities with the polymer, 2D graphene-based materials could be uniformly dispersed in the polymer matrix and promote efficient load transfer from the polymer matrix to the nanomaterials.

Because graphene-based materials appear to be an excellent reinforcement for polymer materials by improving their mechanical properties and enhancing their load bearing

abilities, they have been directed toward tissue engineering applications. Li *et al.* synthesized flexible and fluorescent crosslinked chitosan scaffolds reinforced with GO for tissue engineering applications. Their results demonstrate that the swelling and degradation of the scaffolds was entirely based on the percentage of the GO loaded.<sup>95</sup> Yang *et al.* used GO to fabricate 3D porous scaffold and showed that the addition of GO resulted in uniform pore structures with a higher pore density.<sup>96</sup> Apart from enhancing the mechanical properties of the scaffold, the higher surface area of GO provided higher intermolecular interactions with the cell culture media and enriched the growth, differentiation and proliferation of the cells on the scaffold.<sup>97</sup>

Recently, GO loaded poly L-lysine (PLL) thin films served as an adhesive layer to stack multiple layers of cardiac cells.<sup>98</sup> Surface charges play an important role in growth and differentiation of the cells adsorbed on the surface of the scaffold. Tu *et al.* studied the effect of surface charge on the growth and branching of neuronal cells. Their results demonstrate that selective coating on the GO surfaces varied the neurite length and branching of the neuronal cells.<sup>99</sup> An *et al.* designed a poly(lactic acid)/polyurethane polymer matrix loaded with GO for antimicrobial applications. Their results showed 100% reduction in bacterial cell growth with just 5 wt% of GO in the matrix without any effect on normal human cell lines.<sup>100</sup>

Owing to their exceptional optical properties in the near-IR region, higher surface area and high drug loading capabilities, graphene-based nanomaterials were selected as excellent nanocarrier systems for drug delivery applications. Most of the efficient drugs for cancer therapy suffer from reduced therapeutic efficacy due to their hydrophobicity and easy elimination from the host before reaching the targeted site. Graphene-based nanomaterials emerged as an excellent solution to this problem. Most of the hydrophobic drugs, such as doxorubicin (DOX), paclitaxel, and dexamethasone, were attached onto the surface of the graphene surface by either hydrophobic interactions or  $\pi$ - $\pi$  stacking with the graphene surface. Zhou *et al.* synthesized an efficient pH responsive drug delivery system, where the drug, namely, DOX, was released from the carrier system based on a charge reversal poly electrolyte under acidic conditions.<sup>101</sup> Chowdhury *et al.* synthesized ligand-free graphene nanoribbons loaded DOX for cancer therapy.<sup>102</sup> Their results suggested that Gnrbs were preferentially taken up by the cells that express epidermal growth factor receptors and regulated by the papillomavirus E5 protein.<sup>102</sup> Having exceptional electrical conductivity, graphene-based nanomaterials could tune drug release. Weaver *et al.* synthesized polypyrrole-coated GO nanosheets to channelize the release of dexamethasone from the carrier. Their results showed 100% ON/OFF voltage gated drug release with no passive diffusion of the drug from the polymer matrix.<sup>103</sup> Though graphene-based composites have been investigated as a suitable carrier, they often suffer from  $\pi$ - $\pi$  interactions with neighboring molecules, which leads to aggregation and instability. Swain *et al.* explored the effect of a polymer coating on the surface of GO with respect to its stability. Upon surface functionalization with

polyvinylpyrrolidone (PVP) crosslinked poly(vinyl alcohol) (PVA), GO displayed a stability of over 27 months.<sup>104</sup> Swain and Chen *et al.* compared the efficiency of rGO systems over GO for drug delivery applications. Their results showed a two-fold increase in drug loading in rGO compared to that in GO due to the conservation of aromatic structure, which improved the surface area for the drug molecules to be loaded by  $\pi$ - $\pi$  interactions.<sup>105</sup> Another interesting study was based on using rGO-chitosan nanocomposites for microneedle-based transdermal drug delivery applications. Justin *et al.* demonstrated that the effect of drug loading and release was based on the amount of rGO loaded in the composite. Moreover, their results demonstrated that the synthesized materials were susceptible to withhold the tissue insertion and were able to deliver drugs to the epidermis.<sup>106</sup>

Current advancements in technology and science have facilitated the use of graphene-based materials for photothermal therapy in the near-IR region. Graphene, similar to gold nanoparticles and CNTs, absorb the near-IR radiations and efficaciously convert them to thermal vibrations; thus, they can thermally ablate the targeted tissue. Because the human body lacks chromophores that can absorb in the near-IR region, near-IR radiation can access tumor sites with deeper penetration (low scattering) compared to other high energy radiations. Markovic *et al.* compared the photothermal efficiency of GO sheets and carbon nanotubes.<sup>107</sup> A one-fold increase observed in the photothermal properties of graphene sheets over CNTs was attributed to their ultra-small size and uniform dispersion, unlike CNTs, which tend to aggregate when loaded in the polymer matrix. Siriviriyun *et al.* explored the use of GO as a photosensitizer for photodynamic therapy. Their results exhibited a two-photon fluorescence imaging of the cancer cells with photocytotoxicity at a wavelength of 780 nm.<sup>108</sup> Li *et al.* loaded iron oxide nanoparticles in a poly lactic acid matrix, which was surface coated with GO and used them as a hyperthermic and imaging contrast agent for ultrasound, photoacoustic and MR imaging.<sup>109</sup> Nguyen *et al.* also explored the use of near-IR absorption properties of GO for its use as two-photon and photoacoustic imaging agent.<sup>110</sup>

Recently, considerable focus has been given to the use of graphene and graphene-based materials for biosensor applications. Their high electron transport mobility, unprecedented mechanical strength, excellent thermal and electrical conductivity make them appropriate materials for biosensors. The ease of surface functionalization provides high sensitivity, selectivity and stimuli responsive characteristics to the biosensors. Graphene-based electrodes increase the surface area, which helps in increasing the detection limit with a dynamic linear range. Recently, Ouyang *et al.* fabricated a G-PEDOT biosensor for the simultaneous detection of both purines and pyrimidines. The G-PEDOT complex enhanced the surface area, which that led to an amplified electrocatalytic oxidation of DNA bases.<sup>111</sup> Another interesting study was based on using G to lower the  $pK_a$  value of the substrate. Zhou *et al.* fabricated a photoluminescent glucose biosensor, which could preferentially shrink and expand in the presence of glucose. Graphene enhanced the  $pK_a$  value of

Table 3 Polymeric modification of graphene and graphene derivatives and their application

| Graphene/graphene derivatives | Polymer  | Application                | Key results  | Ref. |
|-------------------------------|--|----------------------------|--|------|
| GO                            | Poly L-lysine (PLL)  | 3D tissue engineering      | GO-PLL thin films were used as an adhesion layer between stacked multilayered cardiac cells. Low external electric field endowed the stacked tissue with frequency dependent actuation (open/close) and strong spontaneous tissue beating  | 98   |
| Amine functionalized graphene | Poly pyrrole   | Bio-energy storage devices | Graphene facilitated control and gated release of ATP by electrical stimuli. Graphene functionalization led to an increase in adhesion and mobility of actomyosin with no loss of the actin function upon repeated electrical stimuli  | 115  |
| Graphene                      | Poly( <i>o</i> -phenylenediamine) (PoPD)                                     | Biosensor                  | Adenosine triphosphate (ATP) biosensor with a detection limit of 0.3 nM and dynamic range of 10 nM to 2 mM. The presence of analyte disturbed the interactions between the aptamer and the graphene surface and decreased the current response   | 116  |
| Graphene                      | PEDOT  | Biosensor                  | Biosensors that can simultaneously detect both purines and pyrimidines. Surface area and the conductivity of the film were enhanced after graphene-PEDOT binding   | 111  |
| Graphene                      | Poly(4-vinylphenylboronic acid) (PBA)/ <i>N,N'</i> -methylenebis(acrylamide) | Biosensor                  | Selective and sensitive photoluminescent glucose biosensor that could preferentially fold/unfold in the presence of glucose. Graphene lowered the $pK_a$ value of the PBA group on the electrode surface and preferentially formed bisborate complexes with glucose, which resulted in the shrinking of the micro gels                             | 112  |
| GO/graphene                   | Polyaniline (PANI)   | Biosensors                 | Addition of GO/graphene improved the electrochemical properties, flexibility and specific capacitance of the composite material. Compared to GO-PANI, G-PANI exhibited improved biocompatibility and enhanced cell survival rate   | 117  |
| GO                            | Poly ethylene oxide (PEG)  | Biosensors                 | Fluorescent and positively charged GO-PEG was synthesized. $\pi-\pi^*$ facilitated HUMO-LUMO electronic transition enhanced the fluorescence intensity at lower pH values compared to $n-\pi^*$ assisted electronic transitions at neutral pH. Monitored the growth and metabolism of the cancer cells based on the subtle changes in the local pH | 113  |
| Graphene                      | PEDOT  | Biosensors                 | Graphene and PEDOT hastened the electron transfer between the $H_2O_2$ and hemin. Efficient, stable and selective hydrogen peroxide biosensor with a detection limit of 0.08 mM ranging from $10^7$ to $10^5$ M  | 118  |
| Nitrogen-doped graphene       | Chitosan-poly(styrene sulfonate)   | Biosensors                 | Glucose biosensors were synthesized with a detection limit of 64 $\mu$ M. Loading of nitrogen doped graphene into the matrix increased the capacitive current and decreased the charge transfer resistance of the electrode  | 119  |
| Graphene                      | Poly-(3,4-ethylene dioxythiophene) and polystyrene sulfonate                 | Biosensors                 | Electrochemiluminescence alcohol dehydrogenase biosensor was fabricated with a detection limit of 2.5 $\mu$ M  | 120  |
| Reduced graphene oxide        | Poly(anilineboronic acid) (PABA)   | Biosensors                 | Sialic acid biosensor, where boric acid of PABA preferentially reacts with diols of sialic acid resulting in the formation of an ester after the reaction. A graphene layer dramatically improved the dynamic range and limit of detection of the sensor to 2 $\mu$ M to 1.38 mM and 0.8 $\mu$ M, respectively                                     | 121  |

Table 3 (Contd.)

| Graphene/graphene derivatives   | Polymer   | Application                   | Key results   | Ref. |
|---|---|-------------------------------|---|------|
| Graphene  | PCL   | Biosensors/tissue engineering | Covalent linking of graphene to PCL resulted in homogenous dispersion of graphene in the polymer matrix with enhanced tensile strength and plasticity. 14 times increase in electrical conductivity of the composite with 10% graphene content was observed   | 122  |
| GO  | Poly(3,4-ethylenedioxythiophene) (PEDOT)                            | Biosensors/bioimplants        | Doping of graphene not only enhanced the mechanical properties but also enlarged the active surface area of the electrode. With low impedance, high charge storage capacity, high charge injection limit to perform biocompatible electrical simulation, this could be an excellent material at the electrode-tissue interface  | 114  |
| Graphene  | 58s bioactive glass   | Bone tissue engineering       | Used as a reinforcement for 58s bioactive glass, which improved the compressive strength and fracture toughness of the scaffold with favourable biocompatibility for bone tissue engineering  | 123  |
| Single- and multi-walled GO nanoribbons (SWGONRs, MWGONRs); GO nanoplatelets; single- and multi-walled carbon nanotubes | Polypropylene fumarate  | Bone tissue engineering       | Enhancement in the mechanical properties of the composite compared to pristine polymer. 2D graphene material (SWGONR, MWGONR, and GONP) showed an increase in the mechanical properties compared to 1D graphene materials (SWCNT and MWCNT). Reinforcement was primarily based on the structure (surface area, aspect ratio and crosslinking density) of the nanomaterial | 94   |
| Graphene nanoribbons  | PEG-DSPE (1,2-distearoyl- <i>sn</i> -glycero-3-phosphoethanolamine) | Drug delivery                 | Oxidized graphene nanoribbons provided a higher surface to load doxorubicin on their surface by $\pi$ - $\pi$ stacking. Further coating with DSPE-PEG enhanced their hydrophobicity and showed differential uptake of the drug loaded carrier by the cells that express epidermal growth factor receptors and regulated by human papillomavirus E5 protein                | 102  |
| GO  | Poly( <i>N</i> -vinyl caprolactam) (PVCL)                           | Drug delivery                 | Energy driven endocytosis mediated GO-PVCL nanocarrier delivered camptothecin to cancer cells   | 124  |
| GO nanosheets   | Poly(pyrrole)   | Drug delivery                 | Electrically activated controlled ON/OFF delivery of dexamethasone was achieved. Physical properties of GONS led to the customization of the physiochemical properties and drug loading parameters of the composite film  | 103  |
| GO  | Chitosan  | Drug delivery                 | Apart from enhancing the mechanical properties of the composite film, GO assisted in drug loading and transdermal therapy. The developed micro-needles were able to withstand insertion and were able to penetrate till epidermis and deliver the drug  | 116  |
| GO  | Poly( <i>N</i> -isopropylacrylamide) (pNIPAAm)                      | Drug delivery                 | Thermo- and photoresponsive hydrogel composite microspheres were synthesized. Heat liberated during the photoactivation of GO assisted in the phase transition of pNIPAAm and enabled drug release  | 125  |
| GO  | Poly lactic acid/iron oxide   | Drug delivery                 | Multifunctional iron oxide loaded poly lactic acid microcapsules decorated with GO were synthesized as image-guided photothermal theranostic agent. These conglomerate systems served as contrast agents for ultrasound, MR and photo acoustic imaging  | 109  |

Table 3 (Contd.)

| Graphene/graphene derivatives | Polymer  | Application                      | Key results   | Ref. |
|-------------------------------|--|----------------------------------|---|------|
| GO                            | Hyaluronic acid  | Drug delivery                    | A stable, pH responsive and sustained release drug delivery system was synthesized with higher drug loading capabilities  | 126  |
| GO nanoparticles              | Poly ethylene oxide (PEG)-alginate                       | Drug delivery                    | 3D GONPs were synthesized and functionalized with biocompatible alginate-PEG to deliver doxorubicin <i>via</i> a glutathione mediated drug release  | 127  |
| GO                            | Poly ethylene oxide (PEG)                                | Drug delivery                    | Biocompatible nanocarrier system loaded with paclitaxel to target human lung cancer A549 and human breast cancer MCF-7 cells  | 60   |
| Graphene nanoparticles (GQDs) | Polyvinylpyrrolidone                                     | Drug delivery                    | Smaller sized and highly dispersed graphene nanoparticles outperformed the single-walled carbon nanotubes in photothermal therapy. A two-fold increase in the heat generated by graphene nanoparticles created an oxidative stress and depolarized the mitochondrial membrane, which lead to an apoptosis and necrosis mediated cancer cell death | 107  |
| rGO/GO                        | Poly ethylene oxide (PEG)                                | Drug delivery                    | rGO showed a 3–4 fold enhancement of optical absorption in NIR region compared to GO. Ultra-small size and appropriate surface coating enhanced the blood circulation time of rGO-PEG over GO-PEG. Efficient tumour ablation with ultra-low power of 0.15W cm <sup>-2</sup>   | 105  |
| Mesoporous silica-coated GO   | Polyacrylic acid (PAA)                                   | Drug delivery                    | Higher NIR absorption property of GO facilitated photoacoustic imaging and two photon absorption cross-section for the two-photon imaging sensitive dye   | 110  |
| GO                            | Poly(allylamine)/polyethyleneimine                       | Drug delivery                    | pH responsive charge reversal electrolyte on GO enabled the controlled release of DOX from the carrier  | 111  |
| GO                            | Poly(amido amine) dendrimer                              | Drug delivery                    | Hybrid two-photon photodynamic therapeutics were synthesized that can generate reactive oxygen species under preferential NIR absorption  | 108  |
| Graphene quantum dots         | Polydopamine   | Drug delivery                    | Surface functionalized, stable and nontoxic polydopamine coated graphene quantum dots were synthesized, which could facilitate single cell imaging and be used as an optical contrast agent and drug carrier  | 54   |
| GO/rGO                        | Polyvinylpyrrolidone (PVP) and poly(vinyl alcohol) (PVA) | Drug delivery/tissue engineering | Effect of surface functionalization over the stability of GO is studied. Coating of GO with PVP-PVA provided electrostatic type stabilization for over 27 months  | 114  |
| GO                            | Polyethylenimine   | Gene transfection                | GO-grafted poly ethylene imide as a potential vector for gene delivery enhanced the gene transfection and localization of DNA in the nucleus  | 129  |
| GO                            | Poly L-lysine  | Regenerative medicine            | Layer-by-layer assembly of GO and poly L-lysine showed a significant increase in the growth, differentiation and proliferation of mesenchymal stem cells. Larger surface area and higher intermolecular interactions between the osteogenic media and the GO favoured the osteogenic differentiation of mesenchymal stem cells                    | 97   |
| GO                            | Chitosan   | Tissue engineering               | The addition of GO not only increased the mechanical properties and pore formation but also enhanced the cell proliferation and bioactivity of the chitosan 3D porous scaffold  | 130  |

Table 3 (Contd.)

| Graphene/graphene derivatives              | Polymer   | Application                          | Key results  | Ref. |
|--|---|--------------------------------------|--|------|
| GO   | Poly lactic acid/<br>polyurethane   | Tissue engineering                   | 100% reduction in bacterial growth with just 5% of GO. Excellent antibacterial properties with minimal intrinsic toxicity and no effect on normal cell proliferation and differentiation   | 100  |
| GO nanosheets                              | Poly(acrylic acid)/gelatin  | Tissue engineering                   | Graphene reinforced the poly(acrylic acid)/gelatin hydrogel matrix by improving the mechanical properties (improved tensile strength and elongation at break by 71% and 26%, respectively)   | 131  |
| GO   | Chitosan/hydroxyapatite   | Tissue engineering                   | Enhanced biomineralization by GO–chitosan improved cell adherence, proliferation and elevated the osteoblast function  | 132  |
| GO   | Poly(propylene carbonate) (PPC)   | Tissue engineering                   | 1 wt% of GO enhanced the thermo-mechanical properties of PPC. Super-critical foaming technology was used to prepare 3D porous scaffolds for tissue engineering applications. The addition of GO to the matrix resulted in uniform pore structure with high pore density and small pore size            | 96   |
| GO   | Poly( <i>m</i> -aminobenzene sulfonic acid)/1-polyoxyethylenebis(amine) (NH <sub>2</sub> -PEG-NH <sub>2</sub> ), poly(ethylene glycol) monomethyl ether | Tissue engineering                   | The effects of surface functional charges on the growth and branching of neuronal cells were investigated. Compared to neutral, zwitterionic and negatively charged surfaces, positively charged GO surfaces exhibited enhanced maximum neurite length and branching                                   | 99   |
| GO   | Genipin crosslinked chitosan  | Tissue engineering/<br>drug delivery | Fluorescent and flexible genipin cross-linked chitosan reinforced with GO improved the tensile strength of the material. Swelling behaviour and degree of degradation were governed by the concentrations of GO. Excellent biocompatibility with no systemic toxicity                                  | 95   |
| Multi-walled carbon nanotubes;<br>graphene | Poly(L-lactic acid)   | Tissue engineering                   | The $\pi$ -electron cloud of GO favoured the adsorption of hydrophobic proteins onto the surface of GO. GO nanosheets displayed enhanced cell behaviour compared to fibrous MWCNTs. Graphene-assisted scaffold assisted in enhanced type-1 collagen expression both <i>in vivo</i> and <i>in vitro</i> | 128  |

the substrate and charged the PBA, leading to the formation of a bisborate complex with glucose and inward folding.<sup>112</sup> Zhu *et al.* investigated the enhancement in photoluminescence properties of GO under acidic pH to monitor the growth and proliferation of cancer cells. The positively charged GO–PEG enabled  $\pi$ – $\pi^*$  HOMO–LUMO electronic transitions at lower pH values compared to the  $n$ – $\pi^*$  assisted electronic transitions at neutral pH, which augmented the fluorescence intensity.<sup>113</sup> Tian *et al.* explored the use of a GO–PEDOT composite as an excellent material for the formation of a tissue electrode interface. The doping of GO affords biocompatibility, low impedance, high charge storage capacity, and high charge injection limits for performing electrical simulation.<sup>114</sup> Another interesting application of GO was to use it as a bioenergy storage device. Byun *et al.* synthesized a graphene–polypyrrole hybrid nanostructured

bio energy storage device to manage the release of ATP and control the activity and mobility of actomyosin.<sup>115</sup>

Over the past years, great focus has been given for investigating the biological applications of graphene-based materials. Owing to their exceptional mechanical, optical, electrical and thermal properties, graphene-based materials have been chosen to improve the characteristics of the targeted material. Though graphene-based materials are biocompatible and nontoxic, they often suffer from long term stability. Polymer coatings over the graphene-based materials surmounted this issue by enhancing their stability and improving their biocompatibility. Apart from alleviating the stability of graphene-based materials, apt selection of polymer materials that cover the graphene surface could facilitate diverse biomedical applications (Table 3).

## 4. Toxicology and biosafety of graphene derivative

### 4.1. Recent studies on potential toxicity of graphene derivatives

It is very important to investigate the physicochemical interaction of the nanoparticles with *in vitro* and *in vivo* organelles before applying or considering them for biological application. Because graphene has been primarily considered as an electronic material, many studies have established graphene for

bioapplications such as tissue engineering, drug delivery, and stem cell research. However, extensive observations are required in both *in vivo* and *in vitro* to investigate their cell and biomolecular interactions. Graphene is composed of only carbon atoms; however, GO and graphene quantum dots contain oxygen due to oxidation. Though few *in vitro* and *in vivo* toxicology studies have been reported previously, there has not been much focus on biochemistry and histological impact.<sup>38,133</sup> Therefore, our group has conducted an extensive toxicity evaluation experiment to conduct a deep investigation based on

Table 4 Toxicity of graphene derivatives *in vitro* and *in vivo*

| Graphene derivatives                   | Study                    | Model (cell line/animal)   | Observation  | Ref. |
|--|--------------------------|--|--|------|
| Graphene quantum dots                  | <i>In vitro, in vivo</i> | HeLa cells/female BALB/c mice  | No apparent <i>in vitro</i> and <i>in vivo</i> toxicity of GQD, resulting from its small size and high oxygen content compared with that of the widely used GO-PEG | 132  |
| Graphene quantum dots                  | <i>In vitro, in vivo</i> | KB, MDA-MB231, and A549 cells/BALB/c nude mice   | No acute toxicity or morphological changes of carboxylated GQDs were noted in either system at the tested exposure levels  | 38   |
| GO                                     | <i>In vitro, in vivo</i> | Human fibroblast cells/Kunming mice  | GO may induce severe cytotoxicity and lung diseases  | 134  |
| GO                                     | <i>In vivo</i>           | Kunming mice   | Higher dosages of GO showed toxicity in mice organs  | 135  |
| GO                                     | <i>In vitro</i>          | A549 cells   | The effect of GO on A549 cells is dose and size related  | 136  |
| GO                                     | <i>In vitro</i>          | HeLa cells   | GO toxic in HeLa cells   | 137  |
| GO composite                           | <i>In vitro</i>          | <i>Escherichia coli</i> , <i>Bacillus subtilis</i> , <i>Rhodococcus opacus</i> , <i>Cupriavidus metallidurans</i> , CH <sub>4</sub> and NIH 3T3 fibroblast cells | Nano composite shows lower toxic in bacterial and mammalian cells  | 138  |
| Graphene nanoflakes                    | <i>In vitro</i>          | HeLa cells   | Evaluate size-dependent toxicity of graphene nanoflakes  | 139  |
| Graphene oxide nanowalls               | Bacterial activity       | <i>E. coli</i> and <i>S. aureus</i>  | Cell membrane of the bacteria was effectively damaged by the direct contact of the bacteria  | 140  |
| Oxidized graphene nanoribbons          | <i>In vitro</i>          | HeLa, MCF7, SKBR3 and NIH3T3 cells   | Oxidized graphene nanoribbons showed cytotoxic effects more than GO  | 141  |
| GO and carboxyl graphene nanoplatelets | <i>In vitro</i>          | Hep G2 cells   | GO and carboxyl graphene nanoplatelet-treated cells demonstrated toxicity in cancer cells  | 9    |
| Reduced GO                             | <i>In vitro</i>          | Wild-type zebrafish  | Toxicity to zebrafish embryos and sublethal effects on the heart rate, hatching rate, and the length of larvae   | 142  |
| Nano-GO and nano-reduced GO            | <i>In vitro</i>          | U87MG human glioblastoma cells   | Nano-GO and nano-rGO appeared to show similar levels of toxicity on breast cancer cells  | 143  |

biochemical and histological observations in GQDs treated animals. Our observations do not reveal any significant toxicity exerted by GQDs *in vitro* and *in vivo*. GO has several advantages over graphite or graphene, such as its dispersion in aqueous media, which is essential for biological application. GO contains hydrophilic functional groups, which enable chemical modification and functionalization. The *in vivo* studies using GO are based on the appraisal of bioaccumulation and excretion. The route of administration is also one of the important parameters to be considered in the case of the toxicity of nanomaterials. Due to the increasing importance of GO, there is a need for more detailed and accurate *in vitro* and *in vivo* studies regarding the toxicity of the GO. Wang *et al.* reported that GO could induce dose- and time-dependent cytotoxicity and can also enter into the cytoplasm and nucleus, decreasing cell adhesion, inducing cell floating and apoptosis.<sup>134–136</sup> Another group reported that GO shows less toxicity in fibroblast HeLa cells over other carbon materials such as multi-wall carbon nanotube and nano diamond.<sup>137</sup> In addition to GO, GO-based polymer nanocomposites were also found to show toxicity on bacterial cells.<sup>138</sup> The size-dependent toxicity of graphene nanoflakes were investigated using a cell-based electrochemical impedance sensor, which depends on an interdigitated ITO electrode. Their results showed that the increased toxicity with smaller graphene nanoflakes can be used for electrochemical impedance sensing, optical imaging of cells, and bioassays.<sup>139</sup> Another graphene derivative, graphene nano-walls, posed greater toxicity upon their contact with the bacterial cell membrane leading to the efflux of RNA from the cells. GO and some of its derivatives, such as oxygenated and carboxylated GO nanomaterials showed toxicity in human cancer cells by an MTT assay.<sup>9,141</sup> Zebrafish is considered as one of the most used animal models to evaluate the *in vivo* toxicity of graphene-related materials. One of the research groups reported that MWCNTs, GO, and reduced GO do not show high toxicity to zebrafish embryos, but had some sub-lethal effects on their heart rate, hatching rate, and the length of their larvae.<sup>142</sup> Nano-size GO and reduced GO showed lower toxicity in biomedical areas with higher photothermal effects (Table 4).<sup>143</sup>

#### 4.2. Biological effect of graphene derivatives

Though not many, important studies have been conducted to understand the mechanism of interaction between graphene and biomolecules, especially intracellular organelles. The study reported by Li *et al.* showed that the commercially available pristine graphene increased the generation of reactive oxygen species (ROS) and decreased mitochondrial membrane potential, thus greatly affecting the immune system.<sup>144</sup> As pristine graphene increases intracellular ROS, it triggers apoptosis through a mitochondrial pathway. In this study, authors selected murine RAW 264.7 and demonstrated macrophages triggered cell death, which was evaluated by cell signaling pathways such as the MAPKs and TGF-beta-related pathways.<sup>144</sup> Another report includes the biological effects of pristine graphene in primary murine and immortalized macrophages. The investigation reported that the secretion of cytokines (Th1/Th2,

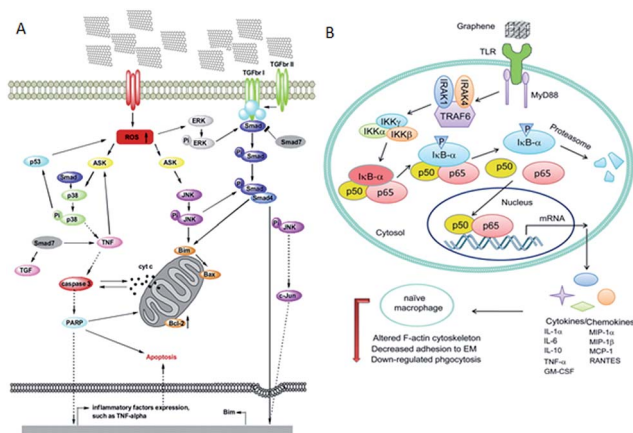


Fig. 5 (A) Signalling pathway of cell apoptosis involved in pristine graphene. This scheme shows that cell apoptosis is caused through ROS-activated MAPKs and TGF-beta pathways. (B) Signalling pathway of macrophage activation stimulated by graphene nano-sheets. Figure adapted from ref. 144 and 145, respectively. Copyright © (2012), with permission from Elsevier.

IL-1 $\alpha$ , IL-6, IL-10, TNF- $\alpha$  and GM-CSF) and chemokines (MCP-1, MIP-1 $\alpha$ , MIP-1 $\beta$  and RANTES) were increased due to pristine graphene.<sup>145</sup> The observations revealed that the graphene activated the TLR-mediated and NF- $\kappa$ B dependent transactions. The report also demonstrated that the graphene remodeled actin assembly, thus altering the morphology of native macrophages and resulted in cells losing their adherence with the extracellular matrix. Though the *in vitro* studies in primary cells demonstrated that graphene induced apoptosis and attenuated phagocytosis, *in vivo* studies are required to obtain comprehensive information about these limitations (Fig. 5).

## 5. Size and dose dependent therapeutic effect of graphene

Nanoparticles (crystal, semi-crystal, semiconductors or metals) with sizes less than 5 nm mostly and equally accumulate in liver and kidney before finally being excreted through the kidney, whereas previous studies have proved that larger particles accumulate in the liver. Unfortunately, no in-depth investigations have been carried out to understand the effect of larger nanoparticles and their effects in the liver and/or other organs. A very recent and advanced study reported by Volarevic *et al.* demonstrated that larger GQDs with a size of 40 nm are highly accumulated in the liver, which can alleviate immune-mediated liver damage.<sup>146</sup> In addition, the rate of liver accumulation is higher for higher doses (50 mg kg<sup>-1</sup>) compared to the lower doses. Though many previous studies have shown that graphene derivatives, especially GQDs with smaller diameters (5–10 nm), interfere with regular cellular mechanisms through interactions with intracellular pathways and induce apoptosis and reduce immunity, this study on GQDs with larger diameters shows complementary results. Nevertheless, both *in vitro* and *in vivo* studies show that GQDs with diameters of 40 nm play a





Fig. 6 (A–C) Small GQDs (15 nm; 50 mg kg<sup>-1</sup> i.v.) were compared with large GQDs (40 nm; 50 mg kg<sup>-1</sup> i.v.) and conventional immunosuppressant dexamethasone (0.5 mg kg<sup>-1</sup> i.v.) for their ability to reduce serum transaminase (A) and IFN- $\gamma$  levels (B), as well as the liver infiltration of IFN- $\gamma$ -producing CD4<sup>+</sup> and CD8<sup>+</sup> T cells (C). The conventional immunosuppressant dexamethasone (0.5 mg kg<sup>-1</sup> i.v.) for their ability to reduce serum transaminase (D) and IFN- $\gamma$  levels (E), as well as liver infiltration of IFN- $\gamma$ -producing CD4<sup>+</sup> and CD8<sup>+</sup> T cells (F). EEM contour maps (after removing Rayleigh scattering) of GQD (blue lines) and the urine of mice treated with GQD (red lines). The shaded region highlights the overlap of GQD and urine emission (G). Figure was adapted with permission from ref. 146. Copyright © 2014 American Chemical Society.

critical role as a therapeutic agent to be used to treat liver inflammation/hepatitis (Fig. 6).

## 6. Conclusion, challenge and prospects

The as-developed and well characterized GQDs can be used not only for biomedical imaging but also for nanocarrier mediated drug delivery, gene delivery, tissue engineering, stem cell research, photothermal cancer therapy and molecular imaging. GQDs also have promising prospects for application in PL-based biosensor development. However, more basic and broad research is required to optimize the reaction conditions with proper analytical methods to obtain a unified structure of GQDs with better properties. Waste management and utilization of byproducts are the biggest challenges with regards to the large scale production of GQDs by chemical exfoliation methods. Because the synthesis process is conducted in highly acidic media, the acids, such as nitric acid and sulfuric acid, are required to be neutralized by adding excess amount of salts.<sup>1</sup> Therefore, it produces a huge amount of by-products, which is one of the major concerns for scaling-up the production system. Though we have found no significant toxicity of GQDs in biological systems, further elaborate toxicity studies are required to observe the bio-degradation of GQDs in biological systems after administration. Studies are also required to assess if the graphene components interact with genetic molecules such as DNA. GQDs require further long term biosafety studies before they can be considered as biomaterials for drug delivery, gene delivery or even for therapeutic applications. Graphene has several unique and promising properties that facilitate it to be considered for various biomedical applications such as drug delivery, gene delivery, tissue engineering and as a photomedicine that can be considered as a therapeutic agent. Large surface areas and ease of functionalization extend their opportunity as a drug delivery carrier. They are widely accepted as a scaffold in tissue engineering as they impart unique mechanical properties. Optical properties of graphene derivatives facilitate *in vitro* and *in vivo* imaging, which is an emerging research field in biomedical and molecular imaging. A promising discovery of graphene derivatives and their photosensitizing properties unveiled a window to use graphene derivatives as a photomedicine to treat diseases, such as cancer, and wounds. Very recent findings include the application of large graphene nanoparticle as therapeutic agents for treating hepatitis, oxidative stress, apoptosis and autophagy. However, considering the safety issues and hurdles of clinical trials, to obtain an approval for the clinical application of graphene derivatives is time consuming and it is barely possible that graphene-based materials will be available in market for biological application before 2030. Therefore, many studies are required to understand their pharmacokinetics, biodegradability, biocompatibility and acute/chronic toxicity studies before graphene can be considered as a promising material for biomedical applications.

## Acknowledgements

This research was supported by grant (NRF-2010-0021427, NRF-2012R1A2A1A01012042) through the National Research Foundation of Korea (NRF) funded by the Ministry of Education, Science and Technology. The authors also extend their appreciation to the Deanship of Scientific Research at King Saud University, Riyadh, Saudi Arabia for funding the work through the Research Group no. RGP-009.

## References

- 1 S. Goenka, V. Sant and S. Sant, *J. Controlled Release*, 2014, **173**, 75.
- 2 K. S. Novoselov, V. I. Fal'ko, L. Colombo, P. R. Gellert, M. G. Schwab and K. Kim, *Nature*, 2012, **490**, 192.
- 3 A. Servant, A. Bianco, M. Prato and K. Kostarelos, *Bioorg. Med. Chem. Lett.*, 2014, **24**, 1638.
- 4 Z. Liu, S. Tabakman, K. Welsher and H. Dai, *Nano Res.*, 2009, **2**, 85.
- 5 S. Gurunathan, J. W. Han, V. Eppakayala, A. A. Dayem, D. N. Kwon and J. H. Kim, *Nanoscale Res. Lett.*, 2013, **8**, 393.
- 6 V. Georgakilas, M. Otyepka, A. B. Bourlinos, V. Chandra, N. Kim, K. C. Kemp, P. Hobza, R. Zboril and K. S. Kim, *Chem. Rev.*, 2012, **112**, 6156.
- 7 T. Lammel, P. Boisseaux, M. L. Fernandez-Cruz and J. M. Navas, *Part. Fibre Toxicol.*, 2013, **10**, 27.
- 8 S. Bae, H. Kim, Y. Lee, X. Xu, J. S. Park, Y. Zheng, J. Balakrishnan, T. Lei, H. R. Kim, Y. I. Song, Y. J. Kim, K. S. Kim, B. Ozyilmaz, J. H. Ahn, B. H. Hong and S. Iijima, *Nat. Nanotechnol.*, 2010, **5**, 574.
- 9 J. Wu, M. Agrawal, H. A. Becerril, Z. Bao, Z. Liu, Y. Chen and P. Peumans, *ACS Nano*, 2010, **4**, 43.
- 10 Z. Liu, K. Parvez, R. Li, R. Dong, X. Feng and K. Mullen, *Adv. Mater.*, 2015, **27**, 669.
- 11 Z. S. Wu, W. Ren, L. Wen, L. Gao, J. Zhao, Z. Chen, G. Zhou, F. Li and H. M. Cheng, *ACS Nano*, 2010, **4**, 3187.
- 12 Z. S. Wu, K. Parvez, X. Feng and K. Mullen, *Nat. Commun.*, 2013, **4**, 2487.
- 13 Z. S. Wu, K. Parvez, X. Feng and K. Mullen, *J. Mater. Chem. A*, 2014, **2**, 8288.
- 14 X. Yan, X. Cui, B. Li and L. S. Li, *Nano Lett.*, 2010, **10**, 1869.
- 15 K. S. Kim, Y. Zhao, H. Jang, S. Y. Lee, J. M. Kim, K. S. Kim, J. H. Ahn, P. Kim, J. Y. Choi and B. H. Hong, *Nature*, 2009, **457**, 706.
- 16 K. S. Novoselov, D. Jiang, F. Schedin, T. J. Booth, V. V. Khotkevich, S. V. Morozov and A. K. Geim, *Proc. Natl. Acad. Sci. U. S. A.*, 2005, **102**, 10451.
- 17 Y. Hernandez, V. Nicolosi, M. Lotya, F. M. Blighe, Z. Sun, S. De, I. T. McGovern, B. Holland, M. Byrne, Y. K. Gun'Ko, J. J. Boland, P. Niraj, G. Duesberg, S. Krishnamurthy, R. Goodhue, J. Hutchison, V. Scardaci, A. C. Ferrari and J. N. Coleman, *Nat. Nanotechnol.*, 2008, **3**, 563–568.
- 18 G. Eda, G. Fanchini and M. Chhowalla, *Nat. Nanotechnol.*, 2008, **3**, 270.
- 19 K. Parvez, Z. S. Wu, R. Li, X. Liu, R. Graf, X. Feng and K. Mullen, *J. Am. Chem. Soc.*, 2014, **136**, 6083.

- 20 K. Parvez, R. Li, S. R. Puniredd, Y. Hernandez, F. Hinkel, S. Wang, X. Feng and K. Mullen, *ACS Nano*, 2013, **7**, 3598.
- 21 A. Lerf, H. He, M. Forster and J. Klinowski, *J. Phys. Chem. B*, 1998, **102**, 4477.
- 22 J. Moon, J. An, U. Sim, S. P. Cho, J. H. Kang, C. Chung, J. H. Seo, J. Lee, K. T. Nam and B. H. Hong, *Adv. Mater.*, 2014, **26**, 3501.
- 23 D. Chen, W. Chen, L. Ma, G. Ji, K. Chang and J. Y. Lee, *Mater. Today*, 2014, **17**, 184–193.
- 24 M. Bacon, S. J. Bradley and T. Nann, *Part. Part. Syst. Charact.*, 2014, **31**, 415.
- 25 D. Pan, J. Zhang, Z. Li and M. Wu, *Adv. Mater.*, 2010, **22**, 734.
- 26 P. Luo, Y. Qiu, X. Guan and L. Jiang, *Phys. Chem. Chem. Phys.*, 2014, **16**, 19011.
- 27 Y. Feng, J. Zhao, X. Yan, F. Tang and Q. Xue, *Carbon*, 2014, **66**, 334.
- 28 M. Zhang, L. Bai, W. Shang, W. Xie, H. Ma, Y. Fu, D. Fang, H. Sun, L. Fan, M. Han, C. Liu and S. Yang, *J. Mater. Chem.*, 2012, **22**, 7461.
- 29 A. Ananthanarayanan, X. Wang, P. Routh, B. Sana, S. Lim, D.-H. Kim, K.-H. Lim, J. Li and P. Chen, *Adv. Funct. Mater.*, 2014, **24**, 3021.
- 30 C. M. Luk, B. L. Chen, K. S. Teng, L. B. Tang and S. P. Lau, *J. Mater. Chem. C*, 2014, **2**, 4526.
- 31 L. A. Ponomarenko, F. Schedin, M. I. Katsnelson, R. Yang, E. W. Hill, K. S. Novoselov and A. K. Geim, *Science*, 2008, **320**, 356–358.
- 32 S. Zhuo, M. Shao and S. T. Lee, *ACS Nano*, 2012, **6**, 1059–1064.
- 33 J. Lu, P. S. Yeo, C. K. Gan, P. Wu and K. P. Loh, *Nat. Nanotechnol.*, 2011, **6**, 247.
- 34 Y. Dong, C. Chen, X. Zheng, L. Gao, Z. Cui, H. Yang, C. Guo, Y. Chi and C. M. Li, *J. Mater. Chem.*, 2012, **22**, 8764.
- 35 M. Nurunnabi, Z. Khatun, G. R. Reeck, D. Y. Lee and Y. K. Lee, *ACS Appl. Mater. Interfaces*, 2014, **6**, 12413.
- 36 K. Chen and X. Chen, *Curr. Top. Med. Chem.*, 2010, **10**, 1227.
- 37 K. K. Alharbi and Y. A. Al-Sheikh, *Saudi J. Biol. Sci.*, 2014, **21**, 109.
- 38 L. B. Josefsen and R. W. Boyle, *Theranostics*, 2012, **2**, 916.
- 39 W. P. Steward and K. Brown, *Br. J. Cancer*, 2013, **109**, 1.
- 40 L. Fass, *Mol. Oncol.*, 2008, **2**, 115.
- 41 Z. Khatun, M. Nurunnabi, K. J. Cho and Y. K. Lee, *ACS Appl. Mater. Interfaces*, 2012, **4**, 3880.
- 42 Z. Khatun, M. Nurunnabi, K. J. Cho and Y. K. Lee, *Carbohydr. Polym.*, 2012, **90**, 1461.
- 43 M. Nurunnabi, K. J. Cho, J. S. Choi, K. M. Huh and Y. K. Lee, *Biomaterials*, 2010, **31**, 5436.
- 44 J. S. Kim, K. J. Cho, T. H. Tran, M. Nurunnabi, T. H. Moon, S. M. Hong and Y. K. Lee, *J. Colloid Interface Sci.*, 2011, **353**, 363.
- 45 V. Voliani, M. González-Béjar, V. Herranz-Pérez, M. Duran-Moreno, G. Signore, J. M. Garcia-Verdugo and J. Pérez-Prieto, *Chem.–Eur. J.*, 2013, **19**, 13538–13546.
- 46 V. Voliani, M. Gemmi, L. Francés-Soriano, M. González-Béjar and J. Pérez-Prieto, *J. Phys. Chem. C*, 2014, **118**, 11404.
- 47 C. Wang, L. Cheng and Z. Liu, *Theranostics*, 2013, **3**, 317–330.
- 48 N. Larson and H. Ghandehari, *Chem. Mater.*, 2012, **24**, 840.
- 49 D. M. Close, T. Xu, G. S. Sayler and S. Ripp, *Sensors*, 2011, **11**, 180.
- 50 S. Gurunathan, J. Woong Han, E. Kim, D. N. Kwon, J. K. Park and J. H. Kim, *J. Nanobiotechnol.*, 2014, **12**, 41.
- 51 J. U. Menon, P. Jadeja, P. Tambe, K. Vu, B. Yuan and K. T. Nguyen, *Theranostics*, 2013, **3**, 152.
- 52 M. Nurunnabi, Z. Khatun, G. R. Reeck, D. Y. Lee and Y. K. Lee, *Chem. Commun.*, 2013, **49**, 5079.
- 53 M. Nurunnabi, Z. Khatun, K. M. Huh, S. Y. Park, D. Y. Lee, K. J. Cho and Y. K. Lee, *ACS Nano*, 2013, **7**, 6858.
- 54 M. Nurunnabi, Z. Khatun, M. Nafiujjaman, D. G. Lee and Y. K. Lee, *ACS Appl. Mater. Interfaces*, 2013, **5**, 8246.
- 55 U. Dembereldorj, M. Kim, S. Kim, E.-O. Ganbold, S. Y. Lee and S.-W. Joo, *J. Mater. Chem.*, 2012, **22**, 23845.
- 56 D. Depan, J. Shah and R. D. K. Misra, *Mater. Sci. Eng., C*, 2011, **31**, 1305.
- 57 Y. Yang, Y. M. Zhang, Y. Chen, D. Zhao, J. T. Chen and Y. Liu, *Chemistry*, 2012, **18**, 4208.
- 58 X. Yang, X. Zhang, Y. Ma, Y. Huang, Y. Wang and Y. Chen, *J. Mater. Chem.*, 2009, **19**, 2710.
- 59 X. Yang, Y. Wang, X. Huang, Y. Ma, Y. Huang, R. Yang, H. Duan and Y. Chen, *J. Mater. Chem.*, 2011, **21**, 3448.
- 60 Z. Xu, S. Wang, Y. Li, M. Wang, P. Shi and X. Huang, *ACS Appl. Mater. Interfaces*, 2014, **6**, 17268.
- 61 M. Wojtoniszak, K. Urbas, M. Peruzńska, M. Kurzawski, M. Drożdżik and E. Mijowska, *Chem. Phys. Lett.*, 2013, **568–569**, 151.
- 62 V. K. Rana, M.-C. Choi, J.-Y. Kong, G. Y. Kim, M. J. Kim, S.-H. Kim, S. Mishra, R. P. Singh and C. S. Ha, *Macromol. Mater. Eng.*, 2011, **296**, 131.
- 63 B. Tian, C. Wang, S. Zhang, L. Feng and Z. Liu, *ACS Nano*, 2011, **5**, 7000.
- 64 P. Huang, C. Xu, J. Lin, C. Wang, X. Wang, C. Zhang, X. Zhou, S. Guo and D. Cui, *Theranostics*, 2011, **1**, 240.
- 65 X. Sun, Z. Liu, K. Welsher, J. T. Robinson, A. Goodwin, S. Zaric and H. Dai, *Nano Res.*, 2008, **1**, 203.
- 66 Z. Liu, J. T. Robinson, X. Sun and H. Dai, *J. Am. Chem. Soc.*, 2008, **130**, 10876.
- 67 H. Kim, D. Lee, J. Kim, T. I. Kim and W. J. Kim, *ACS Nano*, 2013, **7**, 6735.
- 68 K. Liu, J. J. Zhang, F. F. Cheng, T. T. Zheng, C. Wang and J. J. Zhu, *J. Mater. Chem.*, 2011, **21**, 12034.
- 69 Y. Wang, K. Wang, J. Zhao, X. Liu, J. Bu, X. Yan and R. Huang, *J. Am. Chem. Soc.*, 2013, **135**, 4799.
- 70 Y. Pan, H. Bao, N. G. Sahoo, T. Wu and L. Li, *Adv. Funct. Mater.*, 2011, **21**, 2754.
- 71 J. An, Y. Gou, C. Yang, F. Hu and C. Wang, *Mater. Sci. Eng., C*, 2013, **33**, 2827.
- 72 X. Fan, G. Jiao, L. Gao, P. Jin and X. Li, *J. Mater. Chem. B*, 2013, **1**, 2658.
- 73 T. Chen, H. Yu, N. Yang, M. Wang, C. Ding and J. Fu, *J. Mater. Chem. B*, 2014, **2**, 4979.
- 74 N. Abdullah Al, J. E. Lee, I. In, H. Lee, K. D. Lee, J. H. Jeong and S. Y. Park, *Mol. Pharm.*, 2013, **10**, 3736.
- 75 X. Wang, X. Sun, J. Lao, H. He, T. Cheng, M. Wang, S. Wang and F. Huang, *Colloids Surf., B*, 2014, **122**, 638.

- 76 L. Zhang, Z. Wang, C. Xu, Y. Li, J. Gao, W. Wang and Y. Liu, *J. Mater. Chem.*, 2011, **21**, 10399.
- 77 C. Cha, S. R. Shin, N. Annabi, M. R. Dokmeci and A. Khademhosseini, *ACS Nano*, 2013, **7**, 2891.
- 78 F. Demichelis, S. Schreiter and A. Tagliaferro, *Phys. Rev. B: Condens. Matter Mater. Phys.*, 1995, **51**, 2143.
- 79 Rusli, J. Robertson and G. A. J. Amaratunga, *J. Appl. Phys.*, 1996, **80**, 2998.
- 80 J. Ge, M. Lan, B. Zhou, W. Liu, L. Guo, H. Wang, Q. Jia, G. Niu, X. Huang, H. Zhou, X. Meng, P. Wang, C. S. Lee, W. Zhang and X. Han, *Nat. Commun.*, 2014, **5**, 4596.
- 81 Y. Wang, R. Huang, G. Liang, Z. Zhang, P. Zhang, S. Yu and J. Kong, *Small*, 2014, **10**, 109.
- 82 B. P. Viraka Nellore, A. Pramanik, S. R. Chavva, S. S. Sinha, C. Robinson, Z. Fan, R. Kanchanapally, J. Grennell, I. Weaver, A. T. Hamme and P. C. Ray, *Faraday Discuss.*, 2014, **1**.
- 83 S. R. Chavva, A. Pramanik, B. P. V. Nellore, S. S. Sinha, B. Yust, R. Kanchanapally, Z. Fan, R. A. Crouch, A. K. Singh, B. Neyland, K. Robinson, X. Dai, D. Sardar, Y. Lu and P. C. Ray, *Part. Part. Syst. Charact.*, 2014, **31**, 1252.
- 84 P. Rong, K. Yang, A. Srivastan, D. O. Kiesewetter, X. Yue, F. Wang, L. Nie, A. Bhirde, Z. Wang, Z. Liu, G. Niu, W. Wang and X. Chen, *Theranostics*, 2014, **4**, 229.
- 85 S. Z. Nergiz, N. Gandra, S. Tadepalli and S. Singamaneni, *ACS Appl. Mater. Interfaces*, 2014, **6**, 16395.
- 86 Y. Wang, L. Polavarapu and L. M. Liz-Marzan, *ACS Appl. Mater. Interfaces*, 2014, **6**, 21798.
- 87 U. Dembereldorj, S. Y. Choi, E. O. Ganbold, N. W. Song, D. Kim, J. Choo, S. Y. Lee, S. Kim and S. W. Joo, *Photochem. Photobiol.*, 2014, **90**, 659.
- 88 L. Feng, X. Yang, X. Shi, X. Tan, R. Peng, J. Wang and Z. Liu, *Small*, 2013, **9**, 1989.
- 89 B. Chen, M. Liu, L. Zhang, J. Huang, J. Yao and Z. Zhang, *J. Mater. Chem.*, 2011, **21**, 7736.
- 90 T. Ren, L. Li, X. Cai, H. Dong, S. Liu and Y. Li, *Polym. Chem.*, 2012, **3**, 2561.
- 91 F. Zhi, H. Dong, X. Jia, W. Guo, H. Lu, Y. Yang, H. Ju, X. Zhang and Y. Hu, *PLoS One*, 2013, **8**, e60034.
- 92 A. Paul, A. Hasan, H. A. Kindi, A. K. Gaharwar, V. T. Rao, M. Nikkhah, S. R. Shin, D. Krafft, M. R. Dokmeci, D. Shum-Tim and A. Khademhosseini, *ACS Nano*, 2014, **8**, 8050.
- 93 H. Kim and W. J. Kim, *Small*, 2014, **10**, 117.
- 94 G. Lalwani, A. M. Henslee, B. Farshid, L. Lin, F. K. Kasper, Y. X. Qin, A. G. Mikos and B. Sitharaman, *Biomacromolecules*, 2013, **14**, 900.
- 95 J. Li, N. Ren, J. Qiu, X. Mou and H. Liu, *Int. J. Nanomed.*, 2013, **8**, 3415.
- 96 G. Yang, J. Su, J. Gao, X. Hu, C. Geng and Q. Fu, *J. Supercrit. Fluids*, 2013, **73**, 1.
- 97 W. Qi, W. Yuan, J. Yan and H. Wang, *J. Mater. Chem. B*, 2014, **2**, 5461.
- 98 S. R. Shin, B. Aghaei-Ghareh-Bolagh, X. Gao, M. Nikkhah, S. M. Jung, A. Dolatshahi-Pirouz, S. B. Kim, S. M. Kim, M. R. Dokmeci, X. S. Tang and A. Khademhosseini, *Adv. Funct. Mater.*, 2014, **24**, 6136.
- 99 Q. Tu, L. Pang, Y. Chen, Y. Zhang, R. Zhang, B. Lu and J. Wang, *Analyst*, 2014, **139**, 105.
- 100 X. An, H. Ma, B. Liu and J. Wang, *J. Nanomater.*, 2013, **2013**, 7.
- 101 T. Zhou, X. Zhou and D. Xing, *Biomaterials*, 2014, **35**, 4185.
- 102 S. Mullick Chowdhury, P. Manepalli and B. Sitharaman, *Acta Biomater.*, 2014, **10**, 4494.
- 103 C. L. Weaver, J. M. LaRosa, X. Luo and X. T. Cui, *ACS Nano*, 2014, **8**, 1834.
- 104 A. K. Swain and D. Bahadur, *J. Phys. Chem. C*, 2014, **118**, 9450.
- 105 J. Chen, H. Liu, C. Zhao, G. Qin, G. Xi, T. Li, X. Wang and T. Chen, *Biomaterials*, 2014, **35**, 4986.
- 106 R. Justin and B. Chen, *J. Mater. Chem. B*, 2014, **2**, 3759.
- 107 Z. M. Markovic, L. M. Harhaji-Trajkovic, B. M. Todorovic-Markovic, D. P. Kepic, K. M. Arsinin, S. P. Jovanovic, A. C. Pantovic, M. D. Dramicanin and V. S. Trajkovic, *Biomaterials*, 2011, **32**, 1121.
- 108 A. Siriviriyannun, T. Imae, G. Caldero and C. Solans, *Colloids Surf., B*, 2014, **121**, 469.
- 109 X. D. Li, X. L. Liang, X. L. Yue, J. R. Wang, C. H. Li, Z. J. Deng, L. J. Jing, L. Lin, E. Z. Qu, S. M. Wang, C. L. Wu, H. X. Wu and Z. F. Dai, *J. Mater. Chem. B*, 2014, **2**, 217.
- 110 K. T. Nguyen, S. Sreejith, J. Joseph, T. He, P. Borah, E. Y. Guan, S. W. Lye, H. Sun and Y. Zhao, *Part. Part. Syst. Charact.*, 2014, **31**, 1060.
- 111 X. Ouyang, L. Luo, Y. Ding, B. Liu and D. Xu, *J. Electroanal. Chem.*, 2014, **735**, 51.
- 112 M. Zhou, J. Xie, S. Yan, X. Jiang, T. Ye and W. Wu, *Macromolecules*, 2014, **47**, 6055.
- 113 H. Zhu, L. Gao, X. Jiang, R. Liu, Y. Wei, Y. Wang, Y. Zhao, Z. Chai and X. Gao, *Chem. Commun.*, 2014, **50**, 3695.
- 114 H. C. Tian, J. Q. Liu, D. X. Wei, X. Y. Kang, C. Zhang, J. C. Du, B. Yang, X. Chen, H. Y. Zhu, Y. N. Nuli and C. S. Yang, *Biomaterials*, 2014, **35**, 2120.
- 115 K. E. Byun, D. S. Choi, E. Kim, D. H. Seo, H. Yang, S. Seo and S. Hong, *ACS Nano*, 2011, **5**, 8656.
- 116 W. Wen, T. Bao, J. Yang, M. Z. Zhang, W. Chen, H. Y. Xiong, X.-H. Zhang, Y. D. Zhao and S. F. Wang, *Sens. Actuators, B*, 2014, **191**, 695.
- 117 X. Yan, J. Chen, J. Yang, Q. Xue and P. Miele, *ACS Appl. Mater. Interfaces*, 2010, **2**, 2521.
- 118 W. Lei, L. Wu, W. Huang, Q. Hao, Y. Zhang and X. Xia, *J. Mater. Chem. B*, 2014, **2**, 4324.
- 119 M. M. Barsan, M. David, M. Florescu, L. Tugulea and C. M. Brett, *Bioelectrochemistry*, 2014, **99**, 46.
- 120 Y. Gao, J. Li, X. Yang, Q. Xiang and K. Wang, *Electroanalysis*, 2014, **26**, 382.
- 121 Y. Zhou, H. Dong, L. Liu, J. Liu and M. Xu, *Biosens. Bioelectron.*, 2014, **60**, 231.
- 122 S. Sayyar, E. Murray, B. C. Thompson, S. Gambhir, D. L. Officer and G. G. Wallace, *Carbon*, 2013, **52**, 296.
- 123 C. Gao, T. Liu, C. Shuai and S. Peng, *Sci. Rep.*, 2014, **4**, 4712.
- 124 T. Kavitha, I. K. Kang and S. Y. Park, *Colloids Surf., B*, 2014, **115**, 37.

- 125 N. Lu, J. Liu, J. Li, Z. Zhang, Y. Weng, B. Yuan, K. Yang and Y. Ma, *J. Mater. Chem. B*, 2014, **2**, 3791.
- 126 E. Song, W. Han, C. Li, D. Cheng, L. Li, L. Liu, G. Zhu, Y. Song and W. Tan, *ACS Appl. Mater. Interfaces*, 2014, **6**, 11882.
- 127 X. Zhao, L. Liu, X. Li, J. Zeng, X. Jia and P. Liu, *Langmuir*, 2014, **30**, 10419.
- 128 S. Duan, X. Yang, F. Mei, Y. Tang, X. Li, Y. Shi, J. Mao, H. Zhang and Q. Cai, *J. Biomed. Mater. Res., Part A*, 2014, **103**, 1424.
- 129 L. Feng, S. Zhang and Z. Liu, *Nanoscale*, 2011, **3**, 1252.
- 130 S. Dinescu, M. Ionita, A. M. Pandele, B. Galateanu, H. Iovu, A. Ardelean, M. Costache and A. Hermenean, *Bio-Med. Mater. Eng.*, 2014, **24**, 2249.
- 131 S. Faghihi, A. Karimi, M. Jamadi, R. Imani and R. Salarian, *Mater. Sci. Eng., C*, 2014, **38**, 299.
- 132 D. Depan, T. C. Pesacreta and R. D. K. Misra, *Biomater. Sci.*, 2014, **2**, 264.
- 133 Y. Chong, Y. Ma, H. Shen, X. Tu, X. Zhou, J. Xu, J. Dai, S. Fan and Z. Zhang, *Biomaterials*, 2014, **35**, 5041.
- 134 K. Wang, J. Ruan, H. Song, J. Zhang, Y. Wo, S. Guo and D. Cui, *Nanoscale Res. Lett.*, 2010, **6**, 8.
- 135 X. Zhang, J. Yin, C. Peng, W. Hu, Z. Zhu, W. Li, C. Fan and Q. Huang, *Carbon*, 2011, **49**, 986.
- 136 Y. Chang, S. T. Yang, J. H. Liu, E. Dong, Y. Wang, A. Cao, Y. Liu and H. Wang, *Toxicol. Lett.*, 2011, **200**, 201.
- 137 X. Zhang, W. Hu, J. Li, L. Tao and Y. Wei, *Toxicol. Res.*, 2012, **1**, 62.
- 138 I. E. Mejias Carpio, C. M. Santos, X. Wei and D. F. Rodrigues, *Nanoscale*, 2012, **4**, 4746.
- 139 O. J. Yoon, I. Kim, I. Y. Sohn, T. T. Kieu and N.-E. Lee, *J. Biomed. Mater. Res., Part A*, 2014, **102**, 2288.
- 140 J. Peng, W. Gao, B. K. Gupta, Z. Liu, R. Romero-Aburto, L. Ge, L. Song, L. B. Alemany, X. Zhan, G. Gao, S. A. Vithayathil, B. A. Kaiparettu, A. A. Marti, T. Hayashi, J. J. Zhu and P. M. Ajayan, *Nano Lett.*, 2012, **12**, 844.
- 141 S. Mullick Chowdhury, G. Lalwani, K. Zhang, J. Y. Yang, K. Neville and B. Sitharaman, *Biomaterials*, 2013, **34**, 283.
- 142 X. T. Liu, X. Y. Mu, X. L. Wu, L. X. Meng, W. B. Guan, Y. Q. Ma, H. Sun, C. J. Wang and X. F. Li, *Biomed. Environ. Sci.*, 2014, **27**, 676.
- 143 J. T. Robinson, S. M. Tabakman, Y. Liang, H. Wang, H. S. Casalogue, D. Vinh and H. Dai, *J. Am. Chem. Soc.*, 2011, **133**, 6825.
- 144 Y. Li, Y. Liu, Y. Fu, T. Wei, L. Le Guyader, G. Gao, R. S. Liu, Y. Z. Chang and C. Chen, *Biomaterials*, 2012, **33**, 402.
- 145 H. Zhou, K. Zhao, W. Li, N. Yang, Y. Liu, C. Chen and T. Wei, *Biomaterials*, 2012, **33**, 6933.
- 146 V. Volarevic, V. Paunovic, Z. Markovic, B. Simovic Markovic, M. Misirkic-Marjanovic, B. Todorovic-Markovic, S. Bojic, L. Vucicevic, S. Jovanovic, N. Arsenijevic, I. Holclajtner-Antunovic, M. Milosavljevic, M. Dramicanin, T. Kravic-Stevovic, D. Ciric, M. L. Lukic and V. Trajkovic, *ACS Nano*, 2014, **8**, 12098.